

New Pyrazolobenzothiazine Derivatives as Hepatitis C Virus NS5B Polymerase Palm Site I Inhibitors

Giuseppe Manfroni,[†] Dinesh Manvar,[‡] Maria Letizia Barreca,^{*,†} Neerja Kaushik-Basu,^{*,‡} Pieter Leysen,[§] Jan Paeshuyse,[§] Rolando Cannalire,[†] Nunzio Iraci,[†] Amartya Basu,[‡] Maxim Chudaev,[‡] Claudio Zamperini,^{||} Elena Dreassi,^{||} Stefano Sabatini,[†] Oriana Tabarrini,[†] Johan Neyts,^{*,§} and Violetta Cecchetti[†]

[†]Dipartimento di Scienze Farmaceutiche, Università degli Studi di Perugia, Via A. Fabretti 48, 06123 Perugia, Italy

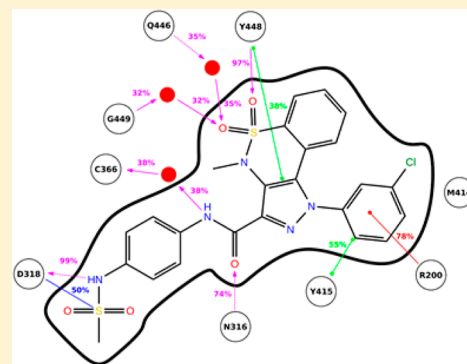
[‡]Department of Biochemistry and Molecular Biology, Rutgers—The State University of New Jersey, 185 South Orange Avenue, New Jersey 07103, United States

[§]Rega Institute for Medical Research, Katholieke Universiteit Leuven, B-3000 Leuven, Belgium

^{||}Dipartimento Biotecnologie, Chimica e Farmacia, Università degli Studi di Siena, Via A. Moro, 53100 Siena, Italy

Supporting Information

ABSTRACT: We have previously identified the pyrazolobenzothiazine scaffold as a promising chemotype against hepatitis C virus (HCV) NSSB polymerase, a validated and promising anti-HCV target. Herein we describe the design, synthesis, enzymatic, and cellular characterization of new pyrazolobenzothiazines as anti-HCV inhibitors. The binding site for a representative derivative was mapped to NSSB palm site I employing a mutant counterscreen assay, thus validating our previous *in silico* predictions. Derivative **2b** proved to be the best selective anti-HCV derivative within the new series, exhibiting a IC_{50} of 7.9 μM against NSSB polymerase and antiviral effect (EC_{50} = 8.1 μM ; EC_{90} = 23.3 μM) coupled with the absence of any antimetabolic effect (CC_{50} > 224 μM ; SI > 28) in a cell based HCV replicon system assay. Significantly, microscopic analysis showed that, unlike the parent compounds, derivative **2b** did not show any significant cell morphological alterations. Furthermore, since most of the pyrazolobenzothiazines tested altered cell morphology, this undesired aspect was further investigated by exploring possible perturbation of lipid metabolism during compound treatment.



INTRODUCTION

Hepatitis C virus (HCV) infection affects approximately 180 million people worldwide and is the main cause of hepatocellular carcinoma and liver transplantation in industrialized countries.^{1,2} Among several infectious diseases, chronic HCV infection is one of the hardest to treat. Currently there is no vaccine against HCV,³ and therapy consists of a NS3/4A protease inhibitor, i.e., boceprevir⁴ or telaprevir,⁵ administered in combination with interferon α (pegIFN- α) and ribavirin (RBV).⁶ This regimen improves the sustained virological response (SVR) to about 70% in the most prevalent HCV genotype in industrialized countries, namely, genotype 1, compared to the standard of care (pegIFN- α and RBV). However, the triple therapy still suffers from additional side effects, high cost, and increased pill burden. Thus, the development of a more adherent and efficacious therapy still remains an unmet medical need. A possibility is a combination of direct-acting antiviral agents (DAAs) targeting different HCV proteins that could eliminate the concomitant use of pegIFN- α and RBV.^{7,8} Almost all the nonstructural proteins (NSs) involved in HCV replication have been extensively

studied and targeted to reach the goal, with several DAAs currently in different stages of clinical trials.^{9,10}

The HCV NSSB RNA-dependent RNA polymerase (RdRp) is a validated and attractive target to identify new DAAs, given its key role in viral replication and significant differences from mammalian polymerases.¹¹ In addition to the active site, NSSB harbors at least five allosteric sites: (i) thumb site I (TSI), (ii) thumb site II (TSII), (iii) palm site I (PSI), (iv) palm site II (PSII), and (v) palm site III (PSIII). NSSB inhibitors are classified as nucleoside inhibitors (NIs) or non-nucleoside inhibitors (NNIs) based on whether they bind to the active site or to one of the five allosteric sites, respectively.^{12–14} Tremendous efforts made by both pharmaceutical companies and academic groups culminated with the identification of DAAs targeting NSSB that are now under clinical evaluation either alone or in combined therapy.^{9,10} Unfortunately, the development of NSSB inhibitors suffers from high attrition rate and none of them has reached the market yet. Thus, the

Received: October 31, 2013

Published: March 21, 2014

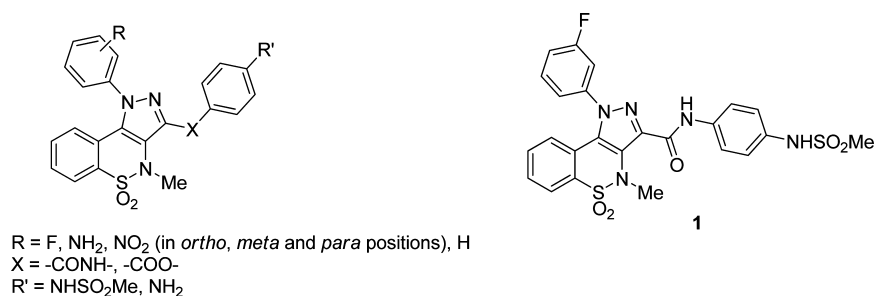
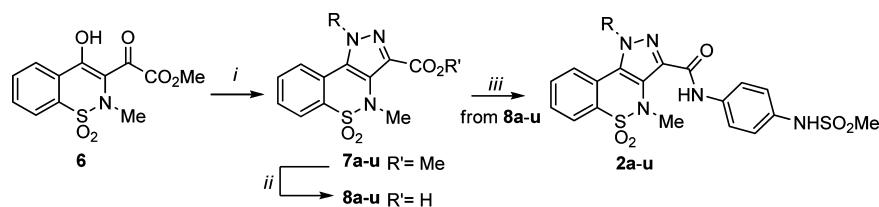


Figure 1. (Left) General formula of our first series of anti-NSSB pyrazolobenzothiazines. (Right) Hit compound 1.

Scheme 1^a



2, 7 and 8	R	2, 7 and 8	R
a	(3-Cl)Ph	l	(3-CF ₃)Ph
b	(4-Cl)Ph	m	(4-CF ₃)Ph
c	(2-Cl)Ph	n	(2-CF ₃)Ph
d	(3-Br)Ph	o	(3,4-diF)Ph
e	(4-Br)Ph	p	(3,4-diCl)Ph
f	(2-Br)Ph	q	(3,4-diMe)Ph
g	(3-Me)Ph	r	(3-Cl, 4-Me)Ph
h	(4-Me)Ph	s	(3-CF ₃ , 4-Cl)Ph
i	(2-Me)Ph	t	Cy
j	(3-OMe)Ph	u	H
k	(4-OMe)Ph		

^aReagents and conditions: (i) ArNHNH₂·HCl or CyNHNH₂·HCl or NH₂NH₂·HCl, MeOH, reflux; (ii) 10% aq NaOH, MeOH, reflux; (iii) (a) SOCl₂, reflux and (b) *N*-(4-aminophenyl)methanesulfonamide, Et₃N, dry DMF, 40 °C.

discovery of new chemotypes able to inhibit NSSB remains of great interest.

In this context, we have directed our efforts toward the identification of new anti-HCV chemotypes acting as NSSB NNIs.^{15–17} Employing a structure-based discovery approach, we recently reported on the identification of a novel series of pyrazolobenzothiazine-based anti-HCV compounds targeting the NSSB polymerase (Figure 1).¹⁷ A preliminary structure–activity relationship (SAR) profiling of this class of NNIs revealed that (i) the best substituent on the *N*-1-phenyl group of the pyrazolobenzothiazine nucleus was the fluorine atom with the *meta* position exhibiting the highest activity; (ii) the methanesulfonamide moiety played an important role, since its replacement with an amino group generated inactive molecules in both the anti-NSSB and anti-HCV replicon assays; (iii) an amide spacer was strongly preferred over an ester linkage. Accordingly, compound 1 (Figure 1) emerged as the most active hit within this first series of pyrazolobenzothiazines.¹⁷

Specifically, docking of compound 1 within PSI revealed that (i) the benzene ring and the *N*-1-phenyl moiety of the pyrazolobenzothiazine nucleus filled two hydrophobic pockets in the PSI; (ii) the sulfonyl function engaged in a direct hydrogen bond with Tyr448 and in a water-mediated interaction with Gly449; (iii) the *p*-methanesulfonamide phenyl

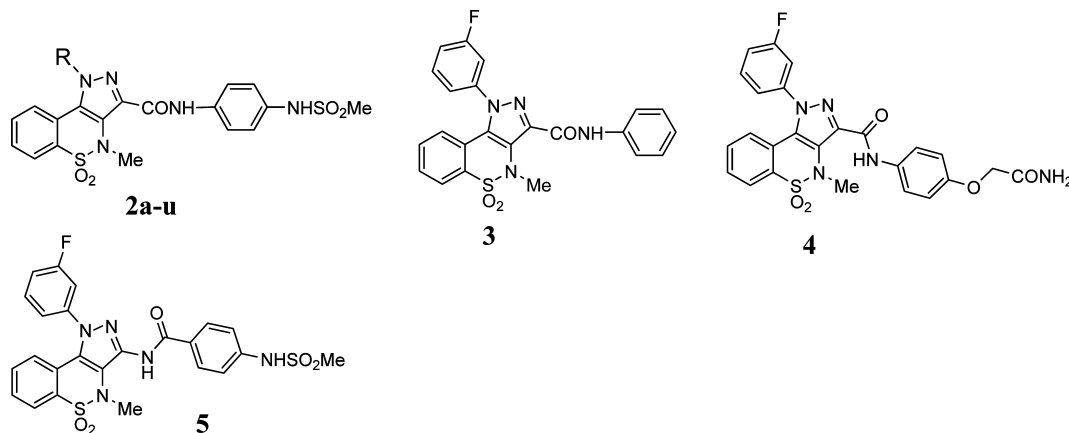
moiety at the C-3 amide group established several polar interactions with the surrounding NSSB residues.¹⁷

On the basis of this analysis, we describe herein the design and synthesis of novel pyrazolobenzothiazine derivatives in an attempt to better outline their SAR profile and optimize their biological activities. Furthermore, we report on the effect of these compounds on HCV NSSB polymerase inhibition and on HCV RNA replication. Employing mutant counterscreen assays, we have investigated the interaction of one of the most potent compounds with the NSSB binding pockets to validate its putative binding site, i.e., PSI. Finally, we describe molecular modeling, *in vitro* ADME, and drug-induced phospholipidosis investigations, aimed at gaining more detailed insight into NSSB pyrazolobenzothiazine inhibitors.

RESULTS AND DISCUSSIONS

Design of the New Pyrazolobenzothiazines. Employing pyrazolobenzothiazine derivative 1 as our reference, we designed and synthesized derivatives 2a–u (Scheme 1 and Table 1) to explore the influence of the interaction of the lipophilic tail at the *N*-1 position with the hydrophobic pocket in the PSI. In particular, we replaced the *m*-fluorine atom of hit 1 with the more lipophilic chlorine (2a) and bromine (2d) substituents and also shifted these two new halogens from the *meta* to the *para* (2b, 2e) and the *ortho* (2c, 2f) positions,

Table 1. Biological Activities of the Target Pyrazolobenzothiazines 2a–u, 3, 4, and 5

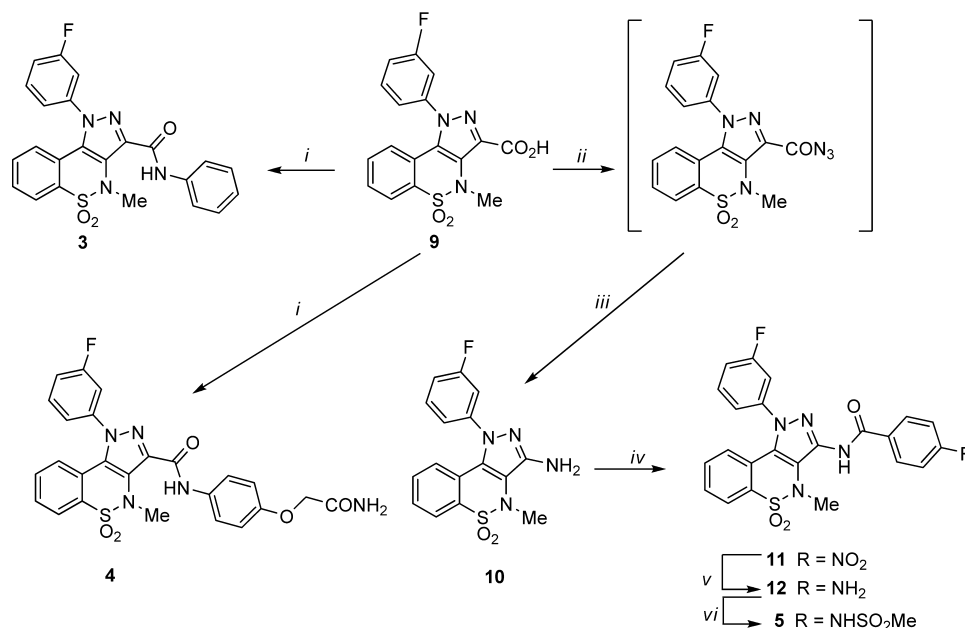


compd	R	anti-NSSB assay, IC ₅₀ ^a (μM)	cell-based replicon assay			
			EC ₅₀ ^b (μM)	EC ₉₀ ^c (μM)	CC ₅₀ ^d (μM)	SI ^e
2a	(3-Cl)Ph	4.3 ± 0.2	9.8 ± 3.2	41 ± 11	>179	>18
2b	(4-Cl)Ph	7.9 ± 0.3	8.1 ± 4.3	23.3 ± 11.4	>224	>28
2c	(2-Cl)Ph	17.8 ± 0.5	7.4 ± 2.1	20.8 ± 3.9	>224	>30
2d	(3-Br)Ph	7.7 ± 0.2	8.3 ± 0.5	26 ± 5	>166	>20
2e	(4-Br)Ph	12.1 ± 0.5	7.4 ± 0.8	21 ± 5	>166	>22
2f	(2-Br)Ph	26.5 ± 3.3	12.0 ± 0.4	ND ^g	107 ± 34	8.9
2g	(3-Me)Ph	21.2 ± 4.5	5.1 ± 0.6	11.8 ± 1.2	>233	>46
2h	(4-Me)Ph	14.7 ± 0.2	4.8 ± 1.7	19.6 ± 11.8	>186	39
2i	(2-Me)Ph	30.8 ± 3.8	14.3 ± 1.1	ND ^g	>233	>16
2j	(3-OMe)Ph	NA ^f	11 ± 2	ND ^g	>181	>16
2k	(4-OMe)Ph	NA ^f	8.1 ± 1.5	25.0 ± 7.3	>226	>28
2l	(3-CF ₃)Ph	23.7 ± 0.9	7.7 ± 1.9	33.2 ± 24.9	>211	>28
2m	(4-CF ₃)Ph	36.3 ± 4.2	7.3 ± 0.8	31.2	>169	>23
2n	(2-CF ₃)Ph	NA ^f	25.0 ± 3	ND ^g	>169	>7
2o	(3,4-diF)Ph	25.4 ± 3.8	13.9 ± 0.4	ND ^g	138 ± 24	9.9
2p	(3,4-diCl)Ph	2.7 ± 0.3	9.7 ± 1.8	ND ^g	>168	>17
2q	(3,4-diMe)Ph	NA ^f	6.2 ± 0.3	20 ± 2	>181	>29
2r	(3-Cl,4-Me)Ph	8.0 ± 1.0	7.0 ± 2.0	37 ± 4	>175	>25
2s	(3-CF ₃ ,4-Cl)Ph	NA ^f	6.4 ± 1.7	ND ^g	>160	>25
2t	Cy	43.0 ± 0.7	4.5 ± 0.6	11 ± 2	44 ± 38	9.7
2u	H	NA ^f	88.2 ± 42.8	65.2	155 ± 50.5	2.5
3		NA ^f	4.5 ± 0.6	ND ^g	56	12
4		NA ^f	15 ± 2	34 ± 7	>192	>13
5		NA ^f	80.8 ± 9.4	ND ^g	160 ± 18.2	2.3
1 ^h	(3-F)Ph	21.0 ± 2.8	7.5 ± 2.5	42.0 ± 2.0	>370	>49

^aIC₅₀ = concentration of compound that inhibits 50% enzyme activity in vitro. The reported values represent the mean ± SD of data derived from two independent experiments performed in duplicate. ^bEC₅₀ = the effective concentration that is required to inhibit virus replication by 50% as quantified by luciferase reporter signal. The reported values represent the mean ± SD of data derived from at least three dose–response curves. ^cEC₉₀ = the effective concentration that is required to inhibit virus replication by 90% as quantified by luciferase reporter signal. The reported values represent the mean ± SD of data derived from at least three independent dose–response curves. ^dCC₅₀ = concentration that is required to reduce the bioreduction of MTS (3-(4,5-dimethylthiazol-2-yl)-5-(3-carboxymethoxyphenyl)-2-(4-sulfophenyl)-2H-tetrazolium) into formazan by 50% and is representative of the antimetabolic effect of the compound on the host cell. The reported value represents the mean ± SD of data derived from at least three dose–response curves. ^eSI = selectivity index (ratio of CC₅₀ to EC₅₀). ^fNA = not active. These compounds were not able to reach ≥50% inhibition of NSSB RdRp activity at 50 μM. ^gND = not determined. These compounds were not able to reach 90% inhibition of HCV replication at any concentration employed. ^hData from ref 17.

respectively. The fluorine atom of **1** was also replaced by other groups with varying degrees of lipophilicity such as methyl (**2g**), methoxy (**2j**), or a trifluoromethyl (**2l**). These groups were also placed in para (**2h**, **2k**, and **2m**) and ortho (**2i**, **2n**) positions, with the exception of the *o*-methoxy group because in this case the requisite starting material was not available by our common suppliers. Further modifications carried out on the N-1 tail of the pyrazolobenzothiazine scaffold entailed the introduction of an additional fluorine atom to obtain the

meta/para-disubstituted fluorine derivative (**2o**). Other disubstitution patterns, selected on the basis of commercially available phenylhydrazines as starting material, were also investigated by designing meta/para-disubstituted derivatives such as dichloro (**2p**), dimethyl (**2q**), chloro/methyl (**2r**), and trifluoromethyl/chloro (**2s**) compounds. Furthermore, the phenyl ring at the N-1 position was either replaced by a cyclohexyl fragment to obtain compound **2t** or completely removed in order to realize the N-1 hydrogen derivative **2u**. In order to

Scheme 2^a

^aReagents and conditions: (i) (a) SOCl_2 , reflux and (b) ArNH_2 , Et_3N , dry DMF, 40°C ; (ii) (a) SOCl_2 , reflux and (b) 1 M aq NaN_3 , acetone, 0°C to rt; (iii) 37% HCl /toluene (1:1), 100°C ; (iv) 4-nitrobenzoyl chloride, dry py, 40°C ; (v) H_2 /Raney Ni, DMF, rt and atm pressure; (vi) MsCl , dry py, dry CH_2Cl_2 , 0°C to rt.

definitively confirm the importance of the methanesulfonamide moiety as an essential pharmacophoric element,¹⁷ it was removed (derivative 3) or replaced by an oxyacetamide fragment (derivative 4) (Scheme 2 and Table 1); the latter substituent has been reported as a suitable group for anti-HCV activity and in vivo properties in the well-known anti-NSSB benzothiadiazine series described in the literature.¹⁸ Finally, with the aim of exploring the influence of the amide on the inhibitory activity of our series of pyrazolobenzothiazine derivatives, it was inverted to give derivative 5 (Scheme 2 and Table 1).

Chemistry. The synthetic pathways utilized in the preparation of the desired pyrazolobenzothiazines 2a–u, and 3–5 are outlined in Schemes 1 and 2, respectively. Through a regioselective condensation¹⁷ of key synthon 6¹⁹ with the appropriate hydrazine hydrochloride, the N-1 phenylpyrazolobenzothiazine esters 7a–c,¹⁹ 7d–g, 7h,¹⁹ 7i–k, 7l,¹⁹ 7m–s, the N-1 cyclohexyl pyrazolobenzothiazine 7t, and the N-1 unsubstituted pyrazolobenzothiazine 7u were prepared and subsequently hydrolyzed under basic conditions. The 3-carboxylic acids 8a–k, 8l,¹⁹ and 8m–u thus obtained were then converted to the corresponding acyl chloride, under reflux of SOCl_2 , and immediately reacted with N-(4-aminophenyl)-methanesulfonamide,²⁰ using Et_3N as scavenger, to obtain the target amide derivatives 2a–u (Scheme 1). Next, by use of the latter procedure, the acid 9¹⁷ (Scheme 2) was reacted with aniline or 2-(4-aminophenoxy)acetamide²¹ to give the target 3 or 4, respectively.

The synthesis of the inverse amide 5 (Scheme 2) entailed the conversion of the 3-carboxylic acid 9¹⁷ into the corresponding unstable azide intermediate which was immediately decomposed to the 3-aminopyrazolobenzothiazine 10 through a Curtius reaction. Derivative 10 was then reacted with *p*-nitrobenzoyl chloride in dry pyridine to afford the nitro intermediate 11, which was reduced under catalytic hydrogenation to the corresponding amino derivative 12. Finally,

mesylation of the latter compound gave the desired target derivative 5.

Anti-NSSB Activity. The anti-NSSB activity of the target compounds 2a–u and 3–5 (Table 1) was determined using recombinant NSSBC Δ 21 1b in a primer dependent elongation assay as described previously (see also Supporting Information).^{16,17,22–24}

All compounds were first screened at $50\ \mu\text{M}$ to identify NSSB inhibitor candidates exhibiting $\geq 50\%$ inhibition of NSSB RdRp activity at this concentration. This investigation led to the identification of 15 compounds (2a–i, 2l, 2m, 2o, 2p, 2r, 2t) satisfying this criterion, while nine compounds (2j, 2k, 2n, 2q, 2s, 2u, 3–5) exhibited at the same concentration lower inhibition of NSSB RdRp activity; the latter compounds were thus considered as inactive.

The fifteen selected compounds were further screened for their NSSB inhibition potency and yielded IC_{50} values ranging from 2.7 to $43\ \mu\text{M}$.

Compounds 2a ($\text{IC}_{50} = 4.3\ \mu\text{M}$), characterized by the presence of a N-1 *m*-chlorophenyl residue, exhibited the highest NSSB inhibitory activity within the monosubstituted derivatives, displaying about 5-fold higher activity than the parent compound 1 ($\text{IC}_{50} = 21.0\ \mu\text{M}$). Further analysis of the monosubstituted miniseries (compounds 2a–n) clearly showed that the meta and para substitutions at the N-1 phenyl ring of the pyrazolobenzothiazine were preferred over the ortho substitution irrespective of the nature of the substituent. In particular, the *m*-chlorine (2a) and *p*-chlorine (2b) derivatives were about 4-fold and 2-fold more active than the corresponding *o*-chlorine derivative 2c, respectively. From a head to head comparison between the *m*-chloro derivative 2a and hit compound 1, it was clear that chlorine was a good replacement for fluorine. This pattern was consistent in the N-1 bromophenyl substituted derivatives 2d–f. The presence of a methyl group (derivatives 2g–i) or a trifluoromethyl group (derivatives 2l and 2m) yielded less active compounds,

although the impact of their positions on the activity was less evident. The presence of a more polar methoxyl group (**2j** and **2k**) resulted in inactive compounds, highlighting the importance of a lipophilic substituent at the N-1 phenyl ring. The importance of the lipophilic and bulky nature of the N-1 substituent was also confirmed by the very low activity shown by N-1 cyclohexyl derivative **2t** and by the totally inactive N-1 unsubstituted derivative **2u**.

The meta/para-disubstituted derivatives designed with the objective to better fill the hydrophobic cavity on NSSB polymerase showed variable activities. In particular, the dichloro and the chloro/methyl N-1 phenyl substituted derivatives **2p** and **2r** exhibited enhanced activity (IC_{50} of 2.7 and 8.0 μ M, respectively), with derivative **2p** representing the best hit in anti-NSSB functional assay. By contrast, the difluoro N-1 phenyl substituted derivative **2o** was less active than compound **1**. These data further demonstrated that chlorine is a good replacement for fluorine at the meta and/or para position.

We previously reported that replacement of the amide linkage with an ester function was detrimental for the anti-NSSB activity.¹⁷ Consistent with this trend, the reverse amide of starting hit **1** yielded the inactive derivative **5**, thus emphasizing the crucial role of this linker for this series of NNIs. In a SAR study on some benzothiazine and benzothiadiazine PSI-NNIs, it was observed that replacement of the methanesulfonyl moiety with the oxyacetamide chain conferred better pharmacological properties while maintaining potent anti-NSSB inhibition.¹⁸ Paradoxically though, derivative **4** bearing an oxyacetamide moiety on the phenyl ring was inactive. Furthermore, as expected because of our previous observations,¹⁷ deletion of the sole methanesulfonamide fragment on the hit compound **1** also yielded the inactive compound **3**.

Mapping the Inhibitor Binding Site on NSSB. In our previous studies, we reported that pyrazolobenzothiazine-based inhibitors should bind NSSB PSI based on molecular docking studies.¹⁷

With the objective of confirming this *in silico* prediction, we carried out the mutant counterscreen assay^{25–27} with **2a** as a representative member of this class of NSSB inhibitors. In this assay, recombinant NSSBC Δ 21 mutant proteins P495L, M423T, and M414T are employed as screens for TSI, TSII, and PSI binders, respectively.^{25–27}

Each of these proteins carries a mutation at an amino acid that is critical for the binding of inhibitors to each of the aforementioned allosteric sites, thus impairing potency of the inhibitor if these residues are involved. Consistent with our hypothesis, the inhibitory potency of compound **2a** was impaired by mutation at M414T residue of NSSB but not with P495L or M423T mutants (Table 2). This was evident

Table 2. NSSB Mutant Inhibition Parameters for Derivative **2a**^a

binding site	NSSB mutant	IC_{50} (μ M)	fold change
PSI	M414T	127.7 \pm 5.5	29.7
TSI	P495L	5.1 \pm 0.3	1.2
TSII	M423T	9.3 \pm 1.5	2.2

^aThe IC_{50} values were evaluated against the indicated NSSB mutants as described for the wild-type NSSB and represents an average \pm SD of two independent experiments in duplicate. Fold change is indicated relative to NSSB WT (IC_{50} = 4.3 μ M).

from the \sim 30-fold higher IC_{50} value against M414T NSSB relative to wild-type NSSB. By contrast, the IC_{50} value of **2a** either remained unchanged or exhibited an approximate 2-fold increase with NSSB mutant P495L or M423T, respectively. These data thus validated our computational predictions and provided evidence for **2a** binding at PSI of NSSB.

In silico simulations were then performed to confirm the binding mode previously proposed for this class of PSI-NNIs.¹⁷ Toward this end, derivative **2a** was submitted to molecular modeling studies. In a recent paper we rationalized the influence of water molecules and protein flexibility on docking studies, putting particular emphasis on the role of specific water molecules found to mediate hydrogen bond interactions of NNIs with residues Gln446 and/or Gly449 in several experimental structures.²⁸

Pyrazolobenzothiazine derivative **2a** was docked into NSSB polymerase (PDB code 3SKE)²⁹ by means of the Glide software,³⁰ yielding a bound pose that was very similar (heavy-atom rmsd of 1.9 Å) to the one we obtained in our previous paper for derivative **1** (Figure 1),¹⁷ a strict analogue of **2a**. The 3SKE crystal structure was chosen as target because in its waterless form it was found to be one of the best performing in docking-based virtual screening simulations.²⁸ We considered the absence of explicit waters a good premise to avoid biasing in the study of water–ligand–protein interactions. The obtained 3SKE/**2a** complex was then submitted to a 10 ns long molecular dynamics (MD) study³¹ with the aim of investigating the binding mode dynamically. From the heavy-atom rmsd analysis, the system was equilibrated after the first 4 ns of simulation, and thus, this equilibration time was not considered in the binding mode analysis.

The binding of **2a** to NSSB is characterized by several interactions (Figure 2). The sulfone group of the exocyclic sulfonamide is engaged in an ion–dipole interaction with the side chain of Asp318, which in turn accepts an H-bond from the sulfonamidic nitrogen. One of the two endocyclic sulfonamide oxygens establishes hydrogen-bonding with the backbone nitrogen of Tyr448, while the other one is engaged in water-mediated interactions with Gln446 and/or Gly449. The amide group of **2a** is involved in two H-bond interactions: a water-mediated one between the backbone oxygen of Cys366 and the amidic nitrogen and a direct one between the amide oxygen and the side chain of Asn316. Furthermore, compound **2a** is involved in three π interactions: the tricyclic system stacks with the aromatic ring of Tyr448, while the *m*-chlorophenyl moiety interacts with the aromatic ring of Tyr415 and the cationic side chain of Arg200.

Replicon System Assays. The target compounds **2a–u** and **3–5** were evaluated for their anti-HCV activity (EC_{50} , EC_{90}) in Huh-5-2 cells carrying a genotype 1b HCV subgenomic replicon (Table 1). The antimetabolic effect (CC_{50}) of the compounds was investigated in parallel employing the 3-(4,5-dimethylthiazol-2-yl)-5-(3-carboxymethoxyphenyl)-2-(4-sulfophenyl)-2H-tetrazolium (MTS) assay. Only compounds that showed \geq 70% inhibition of virus RNA replication without exhibiting any adverse antimetabolic effect at the concentration tested were considered to be endowed with selective anti-HCV activity. In fact, any compound that can induce a cytostatic effect on cell growth could result indirectly in inhibition of HCV subgenomic replicon replication.^{32,33} The selectivity index (SI) was calculated as well to estimate the therapeutic potential of the compounds in this system. Experimental details for the cellular

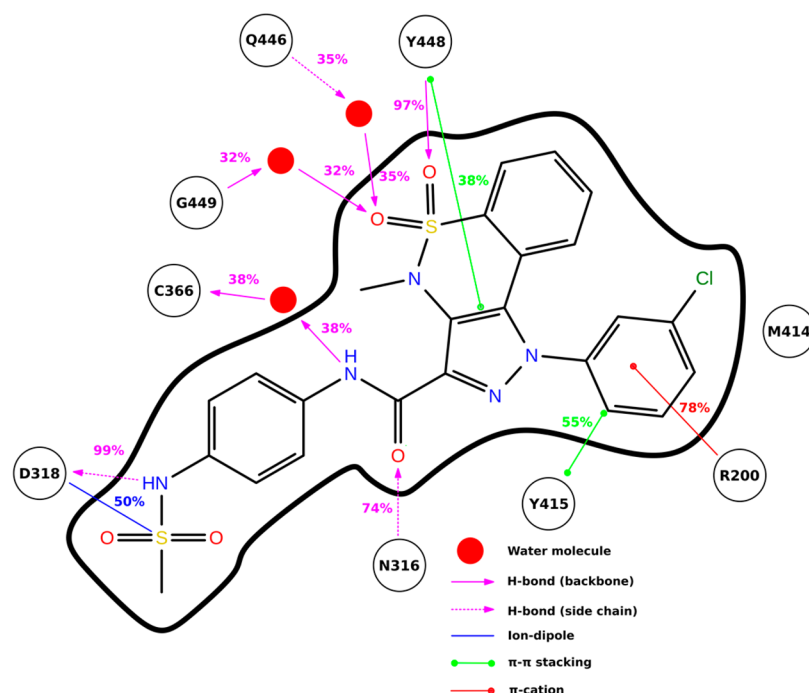


Figure 2. Binding mode analysis of pyrazolobenzothiazine derivative **2a**, depicted together with interacting NSSB residues and water molecules. Main interactions are represented schematically with their occupancies calculated in the time window 4–10 ns.

assays are according to procedures described previously (see also Supporting Information).^{15–17,34}

Furthermore, to identify possible pleiotropic effects exerted by the compounds, the wells were subjected to microscopic examination to discern subtle changes in cellular phenotypes that may have resulted from compound treatment and that could be considered as a hallmark for off-target effects of the compounds.

The cell-based assays (Table 1) revealed that with the exception of derivatives **2n**, **2u**, and **5**, all remaining compounds were active against HCV, displaying EC_{50} values of $\leq 15 \mu\text{M}$. However, because of either a significant toxic effect as apparent from the MTS assay or low SI values (i.e., ≤ 10), compounds **2f**, **2o**, **2t**, and **3** were considered as false positives (EC_{50} not reliable). After dose–response curve analysis, derivatives **2c**, **2i**, **2m**, **2p**, **2r**, **2s**, and **4** were also deemed as unsuitable, as they displayed antimetabolic effect (data not shown). Hence, only derivatives **2a**, **2b**, **2d**, **2e**, **2g**, **2h**, **2k**, **2l** produced selective anti-HCV activity without any antimetabolic effect. After microscopic analysis aimed at visualizing minor changes in the cellular morphology, only pyrazolobenzothiazines **2b**, **2k**, and to less extent **2h** proved to be true anti-HCV agents, as they did not display any significant effects on cell morphology after 72 h of compound treatment. Interestingly, all three of these derivatives were characterized by the presence of a para-substituent at the N-1 phenyl ring. Target compound **2b**, bearing a *p*-chlorine atom on the N-1 phenyl ring, was endowed with comparable inhibitory activity both against NSSB ($IC_{50} = 7.9 \mu\text{M}$) and in cell based HCV replication assay ($EC_{50} = 8.1 \mu\text{M}$ and $EC_{90} = 23.3 \mu\text{M}$). In the case of derivative **2h**, the anti-HCV activity was better than the anti-NSSB activity, but this result can be easily explained by the presence of a slight pleiotropic effect that alters the cellular environment and negatively affects HCV replication. Strangely, compound **2k**, which did not display anti-NSSB activity ($\leq 50\%$ inhibition at

$50 \mu\text{M}$), showed good anti-HCV activity, as is evident from its EC_{50} value of $8.1 \mu\text{M}$ in a cell based assay.

In a head to head comparison, the best selective anti-HCV derivative within this new series (compound **2b**) exhibited equivalent activity as reference compound **1**. Significantly, it is important to note that, unlike the parent compound, derivative **2b** did not exhibit any cell morphological alterations, thus emerging as a more promising antiviral agent.

Selective HCV Inhibition Assessment and Physico-chemical and ADME Properties Characterization. Any compound tested on a HCV replicon system can inadvertently inhibit heterologous elements such as the encephalomyocarditis virus (EMCV) internal ribosome entry site (IRES) or the neomycin phosphotransferase (neo) that is required for the proper translation of the HCV polyprotein or to keep the HCV subgenomic replicon persistently in cells, respectively.³⁵ To explore this unspecific effect in our pyrazolobenzothiazine series, compound **2a** was selected as a representative member because it was one of the best derivatives in both enzymatic and cellular assays and also available in large quantities. Thus, compound **2a** was tested in different replicon systems. On the one hand, we used Huh-9-13 HCV replicons that have the same genetic makeup as Huh-5-2 replicons but differ in (i) their composition of cell culture adaptive mutations, (ii) the absence of a luciferase reporter gene, and (iii) the higher HCV RNA content compared to Huh-5-2 cells. In addition, we employed a subgenomic replicon contained in HuH6 cells, where the replicon has a similar genetic makeup as in Huh-5-2 cells, but (i) it replicates in a different cell line (HuH6 cells instead of Huh-7 cells) and (ii) it carries different adaptive mutations. Moreover, in HCV subgenomic replicon containing HuH6 cells, the replicon replication is not inhibited by IFN- γ and viral RNA replication is independent from cell proliferation.³² Compound **2a** proved to be active in both Huh-9-13 and HuH6 HCV subgenomic replicon bearing cells, exhibiting EC_{50} values of 7.6 and $14 \mu\text{M}$, respectively, as determined by RT-

Table 3. In Vitro Physicochemical and ADME Properties of Derivative 2a

compd	log P^a	water solubility, log S (S in mol L^{-1})		PAMPA-GI, $P_{app} \times 10^{-6}$ (cm/s) (% MR) ^c		HLM ^d (%)
		thermodynamic	kinetic	5 h	22 h	
2a	2.11	-8.40	-6.56	2.30 (7.3)	4.20 (3.2)	99.9

^aLipophilicity was measured through the shake flask method. ^bPermeability assay at different incubation times in gastrointestinal model. ^c% MR: percent membrane retention. ^dMetabolic stability after 60 min in presence of human liver microsomes expressed as percentage of unmodified parent drug.

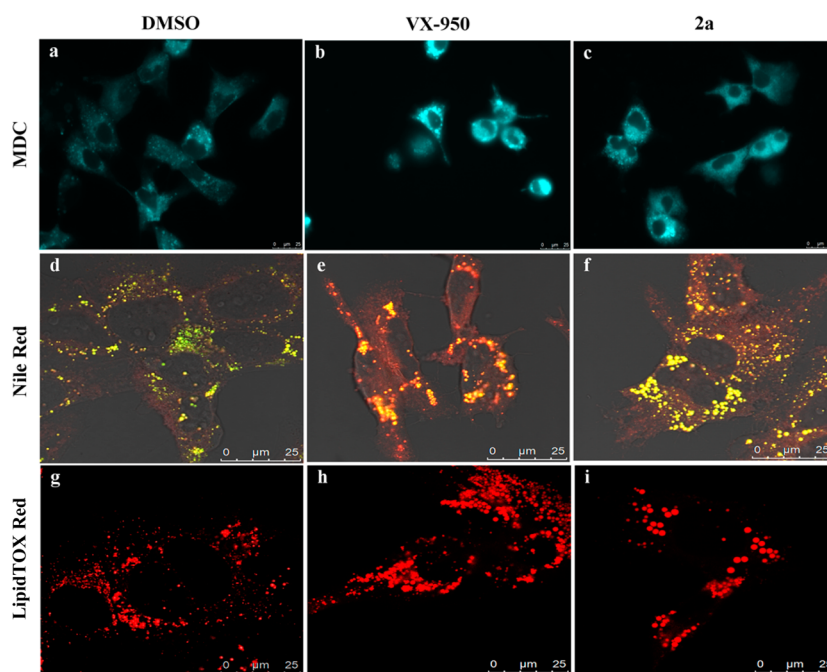


Figure 3. Huh-9-13 cells were stained with monodansylcadaverine (MDC) (a–c), Nile Red (d–f), or LipidTOX red (g–i) after mock treatment (DMSO) or treatment with either the HCV NS3 protease inhibitor VX-950 (at 15 μM) or compound 2a (at 90 μM). Monodansylcadaverine stains multilamellar bodies and autophagic vacuoles (blue). Nile Red stains both neutral lipids (yellow/gold color) and phospholipids (orange/red color). LipidTOX red stains neutral lipids (red).

qPCR. In both replicon containing cells, 2a did not show any effect on the proliferation and metabolism of the host cell as determined by the MTS assay ($CC_{50} > 90 \mu M$). The values obtained are in the same range as for the Huh-5-2 HCV subgenomic replicon containing cells, thus excluding any inhibitory effect on the luciferase expressed by the HCV subgenomic replicons in Huh-5-2 cells.

Derivative 2a was also selected for additional profiling of our pyrazolobenzothiazine PSI-NNIs. Toward this end, log P , thermodynamic and kinetic water solubility (log S), parallel artificial membrane permeability (PAMPA), membrane retention (MR), and human liver microsome (HLM) stability were experimentally determined (Table 3).

The log P value turned out to be in the optimal range for druglike compounds. The thermodynamic solubility value varies with the crystal form of the solid (amorphous, crystalline, different polymorphs, hydrates, and solvates). Kinetic solubility has two distinguishing characteristics: the first one is that the compound initially is fully dissolved in an organic solvent (DMSO) and then added to the water. Desired log S for a drug candidate should be between -4 and -6 , whereas log values of < -6 indicate low solubility. Both low thermodynamic and kinetic solubility values were determined for this derivative, and this behavior may be partially due to a high molecular packing effect. To evaluate membrane permeability, we have used the PAMPA assay proposed by Kansy in 1998.³⁶ Accordingly,

several studies indicate that PAMPA permeability is correlated with both Caco-2 cell permeability and human intestinal absorption.^{37,38} The PAMPA experiments on 2a revealed a low permeability, which cannot be correlated to a high membrane retention as shown by the low MR value. Notably, 2a turned out to be a metabolically stable NSSB inhibitor, given the high HLM stability value, indicating that no metabolites were detected after 60 min of exposure to cytochrome metabolism.

Assessment of Potential Off-Target Effects of the Compounds Studied. As reported in the previous paragraph, microscopic observations had highlighted that, with the exceptions of hit compounds 2b, 2h, and 2k, most of the pyrazolobenzothiazines tested altered cell morphology. These morphological alterations may be a hallmark of potential off-target or pleiotropic effects of the compounds studied. Among the derivatives showing this undesired aspect, compound 2a was selected as a representative analogue for further investigations.

A potential off-target effect observed during compound treatment may due to perturbation of cellular lipid metabolism,³⁹ e.g., inhibition of fatty acid oxidation, which may affect HCV replication.⁴⁰ Candidate drugs can perturb the lipid metabolism of a cell in different ways, for example, by inducing phospholipidosis and steatosis.³⁹ To assess if our pyrazolobenzothiazines could alter the cellular lipid metabolism, we used differential vital stainings that could indicate the ability of

2a to induce phospholipidosis (Nile Red stain and monodansylcadaverine) or drug-induced steatosis (Nile Red stain and LipidTOX red stain). The aim of monodansylcadaverine staining was to screen for the presence of multilamellar bodies, a hallmark of phospholipidosis. Cell treatment with 90 μM derivative **2a** showed that the compound did not induce multilamellar bodies (Figure 3).

Finally LipidTOX red stain and Nile Red stain were performed with the aim to evaluate if compound **2a** was able to induce intracellular accumulation of neutral lipids and/or phospholipids. Overall these two assays demonstrated that derivative **2a** (at 90 μM) significantly altered the neutral lipids content of the treated cells (Figure 3) as apparent from the increase of neutral lipid stain (yellow/gold color) in Nile Red stained cells and the size of the lipid droplets in LipidTOX red stain. These observations suggest that the alteration of cell morphology induced by **2a**, and probably by most of the other pyrazolobenzothiazine derivatives, might be partially due to drug-induced steatosis. A plausible explanation might be the inhibition of mitochondrial β -oxidation by pyrazolobenzothiazines, although other mechanisms of drug-induced steatosis could be equally feasible.⁴¹

In depth analysis of the data obtained by different stainings performed on compound **2b** highlighted that this derivative also induced phospholipidosis/steatosis (i.e., pleiotropic effect) but with an altered effect compared to **2a** (see Supporting Information). Notably, compound **2b** did not show any significant alteration in cell morphology as a consequence of pleiotropic effect at all time points tested.

CONCLUSIONS

We have designed and synthesized novel pyrazolobenzothiazine derivatives with the aim of both tracing a clearer SAR for this class of NSSB NNIs and identifying compounds with improved anti-HCV profile. Biochemical studies and mutant counter-screen assay confirmed that our pyrazolobenzothiazines act as NSSB PSI inhibitors. Most derivatives exhibited EC₅₀ values of $\leq 15 \mu\text{M}$ against HCV in the cell-based replicon assay. Notably, pyrazolobenzothiazine NSSB inhibitors **2b** and **2h** proved to be true anti-HCV agents, as they did not display any antimetabolic and cell morphology alteration effects. Thus, these new derivatives represent an important improvement with respect to the previously reported parent compounds.

A combination of HCV replicons with the same genetic makeup but different cell culture adaptive mutations in several cell types was also employed to understand the effect of compound **2a**, as a representative analogue, on HCV RNA replication, host cell proliferation, and metabolism.

Finally, compound **2a** was also selected among the derivatives showing the undesired pleiotropic effect to assess possible perturbation of cellular lipid metabolism during pyrazolobenzothiazine treatment. Differential staining with dyes such as LipidTOX red and Nile Red revealed that the alteration of cell morphology induced by the pyrazolobenzothiazine **2a** might be partially due to drug-induced steatosis. Additional experimental studies highlighted physicochemical and ADME issues for the representative derivative **2a**.

These findings argue in favor of including phospholipidosis/drug-induced steatosis and pharmacokinetic profile as factors during further chemical optimization of the pyrazolobenzothiazine scaffold to obtain more selective and potent anti-HCV inhibitors and to prevent any side effect of the compounds on hepatic tissue.

EXPERIMENTAL SECTION

Chemistry. Reagents and solvents were purchased from common commercial suppliers and were used as such unless otherwise indicated. Organic solutions were dried over anhydrous Na₂SO₄ and concentrated with a rotary evaporator at low pressure. All reactions were routinely checked by thin-layer chromatography (TLC) on silica gel 60 F254 (Merck) and visualized by using UV or iodine. Column chromatography separations were carried out with Merck silica gel 60 (mesh 70–230). Flash chromatography separations were carried out with Merck silica gel 60 (mesh 230–400). Melting points were determined in capillary tubes (Büchi Electrothermal model 9100) and are uncorrected. Yields were of purified products and were not optimized. ¹H NMR spectra were recorded at 200 or 400 MHz (Bruker Avance DRX-200 or -400, respectively), while ¹³C NMR spectra were recorded at 100 MHz (Bruker Avance DRX-400). Chemical shifts (δ) are given in ppm relative to TMS and calibrated using residual undeuterated solvent as internal reference. Spectra were acquired at 298 K. Data processing was performed with standard Bruker software XwinNMR, and the spectral data are consistent with the assigned structures. The purity of the tested compounds was evaluated by combustion analysis using a Fisons elemental analyzer, model EA1108CHN, and data for C, H, and N are within 0.4% of the theoretical values ($\geq 95\%$ sample purity).

General Procedure for Condensation of Key Intermediate 6 with Hydrazine Hydrochlorides. Method A. A hot solution of the appropriate hydrazine hydrochloride (1.2 mmol) dissolved in hot MeOH (2 mL) was added at once to a refluxing solution of key intermediate **6**¹⁹ (1 mmol) in MeOH (20 mL). The mixture was maintained at reflux for 2–20 h, then concentrated under reduced pressure to half volume and cooled to room temperature. The crystallized solid was filtered under vacuum to give the pyrazolobenzothiazine 3-carboxymethyl esters **7d–g**, **7i–k**, and **7m–u** used as is in the next reaction step.

Methyl 1-(3-Bromophenyl)-4-methyl-1,4-dihydropyrazolo-[4,3-c][1,2]benzothiazine-3-carboxylate 5,5-Dioxide (7d). Following the general procedure method A and using the 3-(bromophenyl)hydrazine hydrochloride, compound **7d** was obtained in 87% yield (reaction time, 15 h) as a whitish amorphous solid: mp 246–248 °C. ¹H NMR (400 MHz, DMSO-*d*₆): δ 3.20 (s, 3H, NCH₃), 3.95 (s, 3H, OCH₃), 7.00 (dd, *J* = 1.6 and 7.6 Hz, 1H, H-9), 7.55–7.60 (m, 2H, H-5' and H-6'), 7.70–7.80 (m, 2H, H-7 and H-8), 7.85–7.90 (m, 2H, H-2' and H-4'), 8.00 (dd, *J* = 1.4 and 7.0 Hz, 1H, H-6).

Methyl 1-(4-Bromophenyl)-4-methyl-1,4-dihydropyrazolo-[4,3-c][1,2]benzothiazine-3-carboxylate 5,5-Dioxide (7e). Following the general procedure method A and using the 4-(bromophenyl)hydrazine hydrochloride, compound **7e** was obtained in 50% yield (reaction time, 3 h) as an orange amorphous solid: mp 196–199 °C. ¹H NMR (400 MHz, DMSO-*d*₆): δ 3.15 (s, 3H, NCH₃), 3.95 (s, 3H, OCH₃), 7.05 (dd, *J* = 1.3 and 7.3 Hz, 1H, H-9), 7.55–7.60 (m, 2H, H-3' and H-5'), 7.65–7.75 (m, 2H, H-7 and H-8), 7.80–7.90 (m, 2H, H-2' and H-6'), 8.00 (dd, *J* = 1.5 and 7.6 Hz, 1H, H-6).

Methyl 1-(2-Bromophenyl)-4-methyl-1,4-dihydropyrazolo-[4,3-c][1,2]benzothiazine-3-carboxylate 5,5-Dioxide (7f). Following the general procedure method A and using the 2-(bromophenyl)hydrazine hydrochloride, compound **7f** was obtained in 90% yield (reaction time, 4 h) as an orange amorphous solid: mp 215–218 °C. ¹H NMR (400 MHz, DMSO-*d*₆): δ 3.20 (s, 3H, NCH₃), 3.95 (s, 3H, OCH₃), 6.75 (d, *J* = 7.9 Hz, 1H, H-9), 7.60–7.75 (m, 4H, H-7, H-8, H-4', and H-5'), 7.85 (d, *J* = 7.7 Hz, 1H, H-6'), 7.95 (d, *J* = 7.8 Hz, 1H, H-3'), 8.00 (d, *J* = 7.7 Hz, 1H, H-6).

Methyl 4-Methyl-1-(3-methylphenyl)-1,4-dihydropyrazolo-[4,3-c][1,2]benzothiazine-3-carboxylate 5,5-Dioxide (7g). Following the general procedure method A and using the 3-(methylphenyl)hydrazine hydrochloride, compound **7g** was obtained in 80% yield (reaction time, 14 h) as a whitish amorphous solid: mp 199–200 °C. ¹H NMR (200 MHz, acetone-*d*₆): δ 2.50 (s, 3H, CH₃), 3.30 (s, 3H, NCH₃), 4.00 (s, 3H, OCH₃), 7.10–7.15 (m, 1H, H-9), 7.35–7.60 (m, 4H, H-2', H-4', H-5', and H-6'), 7.65 (dt, *J* = 1.6 and 7.9 Hz, 1H, H-8), 7.70 (dt, *J* = 1.3 and 7.9 Hz, 1H, H-7), 8.00–8.10 (m, 1H, H-6).

Methyl 4-Methyl-1-(2-methylphenyl)-1,4-dihydropyrazolo[4,3-c][1,2]benzothiazine-3-carboxylate 5,5-Dioxide (7i). Following the general procedure method A and using the 2-(methylphenyl)hydrazine hydrochloride, compound 7i was obtained in 90% yield (reaction time, 10 h) as a whitish amorphous solid: mp 180–182 °C. ¹H NMR (400 MHz, acetone-*d*₆): δ 2.00 (s, 3H, CH₃), 3.30 (s, 3H, NCH₃), 4.00 (s, 3H, OCH₃), 6.85 (d, *J* = 8.0 Hz, 1H, H-9), 7.50–7.65 (m, 5H, H-8, H-3', H-4, H-5', and H-6'), 7.70 (dt, *J* = 1.1 and 7.8 Hz, 1H, H-7), 8.00 (dd, *J* = 0.9 and 7.8 Hz, 1H, H-6).

Methyl 1-(3-Methoxyphenyl)-4-methyl-1,4-dihydropyrazolo[4,3-c][1,2]benzothiazine-3-carboxylate 5,5-Dioxide (7j). Following the general procedure method A and using the 3-(methoxyphenyl)hydrazine hydrochloride, compound 7j was obtained in 60% yield (reaction time, 10 h) as yellow amorphous solid: mp 197–199 °C. ¹H NMR (400 MHz, DMSO-*d*₆): δ 3.13 (s, 3H, NCH₃), 3.75 (s, 3H, OCH₃), 3.90 (s, 3H, CO₂CH₃), 6.95 (dd, *J* = 1.3 and 8.0 Hz, 1H, H-9), 6.95–7.05 (m, 1H, H-4'), 7.13 (t, *J* = 2.1 Hz, 1H, H-2'), 7.15–7.20 (m, 1H, H-6'), 7.50 (t, *J* = 8.1 Hz, 1H, H-5'), 7.65 (dt, *J* = 1.4 and 8.0 Hz, 1H, H-8), 7.70 (dt, *J* = 1.3 and 7.2 Hz, 1H, H-7), 7.90 (dd, *J* = 1.4 and 7.2 Hz, 1H, H-6).

Methyl 1-(4-Methoxyphenyl)-4-methyl-1,4-dihydropyrazolo[4,3-c][1,2]benzothiazine-3-carboxylate 5,5-Dioxide (7k). Following the general procedure method A and using the 4-(methoxyphenyl)hydrazine hydrochloride, compound 7k was obtained in 90% yield (reaction time, 15 h) as a white amorphous solid: mp 206–208 °C. ¹H NMR (400 MHz, acetone-*d*₆): δ 3.25 (s, 3H, NCH₃), 3.90 (s, 3H, OCH₃), 4.00 (s, 3H, CO₂CH₃), 7.15 (dd, *J* = 1.4 and 7.5 Hz, 1H, H-9), 7.20–7.25 (m, 2H, H-3' and H-5'), 7.50–7.55 (m, 2H, H-2' and H-6'), 7.60–7.80 (m, 2H, H-7 and H-8), 8.05 (m, 1H, H-6).

Methyl 4-Methyl-1-[4-(trifluoromethyl)phenyl]-1,4-dihydropyrazolo[4,3-c][1,2]benzothiazine-3-carboxylate 5,5-Dioxide (7m). Following the general procedure method A and using the 4-(trifluoromethylphenyl)hydrazine hydrochloride, compound 7m was obtained in 60% yield (reaction time, 3.5 h) as a white amorphous solid: mp 189–191 °C. ¹H NMR (200 MHz, DMSO-*d*₆): δ 3.20 (s, 3H, NCH₃), 3.90 (s, 3H, OCH₃), 7.10 (dd, *J* = 2.1 and 7.0 Hz, 1H, H-9), 7.65–7.75 (m, 2H, H-7 and H-8), 7.80–7.85 (m, 2H, H-2' and H-6'), 7.95–8.10 (m, 3H, H-6, H-3', and H-5').

Methyl 4-Methyl-1-[2-(trifluoromethyl)phenyl]-1,4-dihydropyrazolo[4,3-c][1,2]benzothiazine-3-carboxylate 5,5-Dioxide (7n). Following the general procedure method A and using the 2-(trifluoromethylphenyl)hydrazine hydrochloride, compound 7n was obtained in 70% yield (reaction time, 4 h) as an orange amorphous solid: mp 222–225 °C. ¹H NMR (400 MHz, DMSO-*d*₆): δ 3.20 (s, 3H, NCH₃), 3.95 (s, 3H, OCH₃), 6.60 (d, *J* = 7.6 Hz, 1H, H-9), 7.60 (dt, *J* = 1.3 and 7.6 Hz, 1H, H-8), 7.70 (dt, *J* = 1.0 and 7.6 Hz, 1H, H-7), 7.80 (d, *J* = 7.2 Hz, 1H, H-3'), 7.95–8.05 (m, 3H, H-4', H-5', and H-6'), 8.10 (dd, *J* = 1.3 and 7.6 Hz, 1H, H-6).

Methyl 1-(3,4-Difluorophenyl)-4-methyl-1,4-dihydropyrazolo[4,3-c][1,2]benzothiazine-3-carboxylate 5,5-Dioxide (7o). Following the general procedure method A and using the 3,4-(difluorophenyl)hydrazine hydrochloride, compound 7o was obtained in 80% yield (reaction time, 4 h) as a white amorphous solid: mp 241–243 °C. ¹H NMR (400 MHz, DMSO-*d*₆): δ 3.15 (s, 3H, NCH₃), 3.90 (s, 3H, OCH₃), 7.10 (dd, *J* = 1.0 and 8.2 Hz, 1H, H-9), 7.40–7.50 (m, 1H, H-6'), 7.65–7.75 (m, 3H, H-7, H-8, and H-5'), 7.85–7.95 (m, 1H, H-2'), 8.05 (dd, *J* = 1.3 and 7.7 Hz, 1H, H-6).

Methyl 1-(3,4-Dichlorophenyl)-4-methyl-1,4-dihydropyrazolo[4,3-c][1,2]benzothiazine-3-carboxylate 5,5-Dioxide (7p). Following the general procedure method A and using the 3,4-(dichlorophenyl)hydrazine hydrochloride, compound 7p was obtained in 80% yield (reaction time, 3 h) as a whitish amorphous solid: mp 300–302 °C. ¹H NMR (400 MHz, DMSO-*d*₆): δ 3.15 (s, 3H, NCH₃), 3.95 (s, 3H, OCH₃), 7.15 (dd, *J* = 1.0 and 7.4 Hz, 1H, H-9), 7.60 (dd, *J* = 2.6 and 8.6 Hz, 1H, H-6'), 7.45–7.55 (m, 2H, H-7 and H-8), 7.85 (d, *J* = 8.6 Hz, 1H, H-5'), 8.00–8.05 (m, 2H, H-6 and H-2').

Methyl 1-(3,4-Dimethylphenyl)-4-methyl-1,4-dihydropyrazolo[4,3-c][1,2]benzothiazine-3-carboxylate 5,5-Dioxide (7q). Following the general procedure method A and using the 3,4-(dimethylphenyl)hydrazine hydrochloride, compound 7q was obtained in 50% yield (reaction time, 4 h) as a whitish amorphous solid:

mp 245–247 °C. ¹H NMR (400 MHz, DMSO-*d*₆): δ 2.20 and 2.30 (s, each 3H, CH₃), 2.75 (s, 3H, NCH₃), 3.90 (s, 3H, OCH₃), 6.95 (dd, *J* = 1.0 and 7.7 Hz, 1H, H-9), 7.20 (dd, *J* = 2.3 and 7.9 Hz, 1H, H-6'), 7.30–7.40 (m, 2H, H-2' and H-5'), 7.55–7.65 (m, 2H, H-7 and H-8), 7.90 (dd, *J* = 1.3 and 6.9 Hz, 1H, H-6).

Methyl 1-(3-Chloro-4-methylphenyl)-4-methyl-1,4-dihydropyrazolo[4,3-c][1,2]benzothiazine-3-carboxylate 5,5-Dioxide (7r). Following the general procedure method A and using the 1-(3-chloro-4-methylphenyl)hydrazine hydrochloride, compound 7r was obtained in 80% yield (reaction time, 4 h) as a whitish amorphous solid: mp 285–287 °C. ¹H NMR (400 MHz, DMSO-*d*₆): δ 2.45 (s, 3H, CH₃), 3.10 (s, 3H, NCH₃), 3.90 (s, 3H, OCH₃), 7.00 (dd, *J* = 1.6 and 7.1 Hz, 1H, H-9), 7.40 (dd, *J* = 2.2 and 8.1 Hz, 1H, H-6'), 7.55 (d, *J* = 8.1 Hz, 1H, H-5'), 7.60–7.65 (m, 3H, H-7, H-8, and H-2'), 7.90 (dd, *J* = 1.6 and 6.8 Hz, 1H, H-6).

Methyl 1-[4-Chloro-3-(trifluoromethyl)phenyl]-4-methyl-1,4-dihydropyrazolo[4,3-c][1,2]benzothiazine-3-carboxylate 5,5-Dioxide (7s). Following the general procedure method A and using the 1-(4-chloro-3-trifluoromethylphenyl)hydrazine hydrochloride, compound 7s was obtained in 50% yield (reaction time, 2 h) as a whitish amorphous solid: mp 291–293 °C. ¹H NMR (400 MHz, DMSO-*d*₆): δ 3.10 (s, 3H, NCH₃), 3.90 (s, 3H, OCH₃), 7.10 (d, *J* = 7.7 Hz, 1H, H-9), 7.60–7.75 (m, 2H, H-7 and H-8), 7.85 (dd, *J* = 2.4 and 8.6 Hz, 1H, H-6'), 7.90 (d, *J* = 8.6 Hz, 1H, H-5'), 8.00 (dd, *J* = 1.0 and 7.3 Hz, 1H, H-6), 8.10 (d, *J* = 2.4 Hz, 1H, H-2').

Methyl 1-Cyclohexyl-4-methyl-1,4-dihydropyrazolo[4,3-c][1,2]benzothiazine-3-carboxylate 5,5-Dioxide (7t). Following the general procedure method A and using the cyclohexylhydrazine hydrochloride, compound 7t was obtained in 50% yield (reaction time, 20 h) as a white solid: mp 198–200 °C. ¹H NMR (200 MHz, acetone-*d*₆): δ 1.25–1.85 (m, 4H, Cy-CH₂), 1.90–2.35 (m, 6H, Cy-CH₂), 3.20 (s, 3H, NCH₃), 3.90 (s, 3H, OCH₃), 4.70–5.00 (m, 1H, Cy-CH), 7.75–7.85 (m, 1H, H-8), 7.90–8.05 (m, 3H, H-6, H-7, and H-9).

Methyl 4-Methyl-1,4-dihydropyrazolo[4,3-c][1,2]benzothiazine-3-carboxylate 5,5-Dioxide (7u). Following the general procedure method A and using the hydrazine hydrochloride, compound 7u was obtained as a yellow solid in 70% yield (reaction time, 5 h) after purification by flash column chromatography, eluting with CH₂Cl₂/MeOH (95:5): mp 218–220 °C. ¹H NMR (200 MHz, DMSO-*d*₆): δ 3.25 (s, 3H, NCH₃), 4.00 (s, 3H, OCH₃), 7.70 (t, *J* = 7.4 Hz, 1H, H-7), 7.80–8.00 (m, 2H, H-8 and H-9), 8.05 (d, *J* = 7.4 Hz, 1H, H-6).

General Procedure of Basic Hydrolysis. Method B. A stirred mixture of appropriate pyrazolobenzothiazine methyl esters 7a–c,¹⁹ 7d–g, 7h,¹⁹ 7i–k, and 7m–u (1 mmol) in aqueous 10% NaOH (6 mL) and MeOH (6 mL) was refluxed for 1 h and then concentrated to one-third of the volume under reduced pressure. The mixture was poured into ice/water and acidified with 2 N HCl (pH 3). The precipitate formed was then filtered under vacuum, washed with Et₂O, and dried to give the pyrazolobenzothiazine-3-carboxylic acids 8a–k, and 8m–u used as is in the next reaction step.

1-(3-Chlorophenyl)-4-methyl-1,4-dihydropyrazolo[4,3-c][1,2]benzothiazine-3-carboxylic Acid 5,5-Dioxide (8a). Following the general procedure method B, compound 8a was obtained from 7a¹⁹ in 85% yield as a white solid: mp 247–248 °C. ¹H NMR (200 MHz, acetone-*d*₆): δ 3.40 (s, 3H, NCH₃), 7.25 (dd, *J* = 0.8 and 6.8 Hz, 1H, H-9), 7.60–7.85 (m, 6H, H-7, H-8, H-2', H-4', H-5', and H-6'), 8.05 (dd, *J* = 1.2 and 7.5 Hz, 1H, H-6).

1-(4-Chlorophenyl)-4-methyl-1,4-dihydropyrazolo[4,3-c][1,2]benzothiazine-3-carboxylic Acid 5,5-Dioxide (8b). Following the general procedure method B, compound 8b was obtained from 7b¹⁹ in 80% yield as a white solid: mp 259–260 °C. ¹H NMR (200 MHz, acetone-*d*₆): δ 3.30 (s, 3H, NCH₃), 7.20–7.25 (m, 1H, H-9), 7.65–7.85 (m, 6H, H-7, H-8, H-2', H-3', H-5', and H-6'), 8.05–8.10 (m, 1H, H-6).

1-(2-Chlorophenyl)-4-methyl-1,4-dihydropyrazolo[4,3-c][1,2]benzothiazine-3-carboxylic Acid 5,5-Dioxide (8c). Following the general procedure method B, compound 8c was obtained from 7c¹⁹ in 75% yield as a white solid: mp 224–226 °C. ¹H NMR (200 MHz, acetone-*d*₆): δ 3.40 (s, 3H, NCH₃), 6.95 (dd, *J* = 1.1 and 6.9 Hz, 1H, H-9), 7.65 (dt, *J* = 1.5 and 6.9 Hz, 1H, H-8), 7.70–7.85 (m, 4H,

H-7, H-3', H-4', and H-5'), 7.90–7.95 (m, 1H, H-6'), 8.05 (dd, $J = 1.5$ and 8.1 Hz, 1H, H-6).

1-(3-Bromophenyl)-4-methyl-1,4-dihydropyrazolo[4,3-c]-[1,2]benzothiazine-3-carboxylic Acid 5,5-Dioxide (8d). Following the general procedure method B, compound 8d was obtained from 7d in 90% yield as a white solid: mp 228–230 °C. $^1\text{H NMR}$ (400 MHz, $\text{DMSO-}d_6$): δ 3.25 (s, 3H, NCH_3), 7.05 (dd, $J = 1.3$ and 7.4 Hz, 1H, H-9), 7.50–7.60 (m, 2H, H-5' and H-6'), 7.65–7.75 (m, 2H, H-7 and H-8), 7.80–7.90 (m, 2H, H-2' and H-4'), 8.00 (dd, $J = 1.7$ and 7.0 Hz, 1H, H-6).

1-(4-Bromophenyl)-4-methyl-1,4-dihydropyrazolo[4,3-c]-[1,2]benzothiazine-3-carboxylic Acid 5,5-Dioxide (8e). Following the general procedure method B, compound 8e was obtained from 7e in 80% yield as a white solid: mp 255–257 °C. $^1\text{H NMR}$ (400 MHz, $\text{DMSO-}d_6$): δ 3.10 (s, 3H, NCH_3), 7.05 (d, $J = 7.5$ Hz, 1H, H-9), 7.50–7.60 (m, 2H, H-3' and H-5'), 7.65–7.80 (m, 2H, H-7 and H-8), 7.80–7.85 (m, 2H, H-2' and H-6'), 8.05 (d, $J = 7.0$ Hz, 1H, H-6).

1-(2-Bromophenyl)-4-methyl-1,4-dihydropyrazolo[4,3-c]-[1,2]benzothiazine-3-carboxylic Acid 5,5-Dioxide (8f). Following the general procedure method B, compound 8f was obtained from 7f in 85% yield as a white solid: mp 274–276 °C. $^1\text{H NMR}$ (400 MHz, $\text{acetone-}d_6$): δ 3.30 (s, 3H, NCH_3), 6.90 (d, $J = 7.6$ Hz, 1H, H-9), 7.60 (dt, $J = 1.2$ and 8.0 Hz, 1H, H-4'), 7.70–7.80 (m, 3H, H-7, H-8, and H-5'), 7.80 (dd, $J = 1.2$ and 6.0 Hz, 1H, H-6'), 7.95 (dd, $J = 1.3$ and 8.0 Hz, 1H, H-3'), 8.00 (dd, $J = 0.7$ and 7.8 Hz, 1H, H-6).

4-Methyl-1-(3-methylphenyl)-1,4-dihydropyrazolo[4,3-c]-[1,2]benzothiazine-3-carboxylic Acid 5,5-Dioxide (8g). Following the general procedure method B, compound 8g was obtained from 7g in 80% yield as a white solid: mp 238–240 °C. $^1\text{H NMR}$ (400 MHz, $\text{acetone-}d_6$): δ 2.50 (s, 3H, CH_3), 3.25 (s, 3H, NCH_3), 7.10 (d, $J = 7.9$ Hz, 1H, H-9), 7.40–7.60 (m, 4H, H-2', H-4', H-5', and H-6'), 7.65 (dt, $J = 1.0$ and 7.6 Hz, 1H, H-8), 7.75 (dt, $J = 1.1$ and 7.6 Hz, 1H, H-7), 8.00 (dd, $J = 1.0$ and 7.6 Hz, 1H, H-6).

4-Methyl-1-(4-methylphenyl)-1,4-dihydropyrazolo[4,3-c]-[1,2]benzothiazine-3-carboxylic Acid 5,5-Dioxide (8h). Following the general procedure method B, compound 8h was obtained from 7h¹⁹ in 80% yield as a white solid: mp 260–261 °C. $^1\text{H NMR}$ (200 MHz, $\text{DMSO-}d_6$): δ 2.40 (s, 3H, CH_3), 3.15 (s, 3H, NCH_3), 7.10 (dd, $J = 1.2$ and 7.0 Hz, 1H, H-9), 7.40–7.80 (m, 4H, H-2', H-3', H-5', and H-6'), 7.80–7.90 (m, 2H, H-7 and H-8), 8.00 (d, $J = 1.2$ and 7.1 Hz, 1H, H-6).

4-Methyl-1-(2-methylphenyl)-1,4-dihydropyrazolo[4,3-c]-[1,2]benzothiazine-3-carboxylic Acid 5,5-Dioxide (8i). Following the general procedure method B, compound 8i was obtained from 7i in 70% yield as a white solid: mp 214–215 °C. $^1\text{H NMR}$ (400 MHz, $\text{acetone-}d_6$): δ 2.00 (s, 3H, CH_3), 3.25 (s, 3H, NCH_3), 6.80 (dd, $J = 1.0$ and 7.0 Hz, 1H, H-9), 7.50–7.60 (m, 5H, H-8, H-3', H-4', H-5', and H-6'), 7.70 (dt, $J = 1.0$ and 7.7 Hz, 1H, H-7), 8.00 (dd, $J = 0.8$ and 7.7 Hz, 1H, H-6).

1-(3-Methoxyphenyl)-4-methyl-1,4-dihydropyrazolo[4,3-c]-[1,2]benzothiazine-3-carboxylic Acid 5,5-Dioxide (8j). Following the general procedure method B, compound 8j was obtained from 7j in 90% yield as a whitish solid: mp 202–204 °C. $^1\text{H NMR}$ (400 MHz, $\text{DMSO-}d_6$): δ 3.10 (s, 3H, NCH_3), 3.80 (s, 3H, OCH_3), 6.90 (d, $J = 7.6$ Hz, 1H, H-9), 7.05 (dd, $J = 1.7$ and 7.4 Hz, 1H, H-4'), 7.15 (t, $J = 2.2$ Hz, 1H, H-2'), 7.20 (dd, $J = 2.2$ and 8.2 Hz, 1H, H-6'), 7.50 (t, $J = 8.2$ Hz, 1H, H-5'), 7.55–7.65 (m, 2H, H-7 and H-8), 7.90 (dd, $J = 1.0$ and 7.8 Hz, 1H, H-6).

1-(4-Methoxyphenyl)-4-methyl-1,4-dihydropyrazolo[4,3-c]-[1,2]benzothiazine-3-carboxylic Acid 5,5-Dioxide (8k). Following the general procedure method B, compound 8k was obtained from 7k in 90% yield as a whitish solid: mp 244–245 °C. $^1\text{H NMR}$ (200 MHz, $\text{acetone-}d_6$): δ 3.30 (s, 3H, NCH_3), 3.95 (s, 3H, OCH_3), 7.10 (dd, $J = 1.3$ and 7.7 Hz, 1H, H-9), 7.20–7.30 (m, 2H, H-3' and H-5'), 7.55–7.60 (m, 2H, H-2' and H-6'), 7.65 (dt, $J = 1.4$ and 7.7 Hz, 1H, H-8), 7.75 (dt, $J = 1.3$ and 7.6 Hz, 1H, H-7), 8.05 (dd, $J = 1.4$ and 7.6 Hz, H-6).

4-Methyl-1-[4-(trifluoromethyl)phenyl]-1,4-dihydropyrazolo[4,3-c][1,2]benzothiazine-3-carboxylic Acid 5,5-Dioxide (8m). Following the general procedure method B, compound 8m was obtained from 7m in 90% yield as a whitish solid: mp 187–189

°C. $^1\text{H NMR}$ (400 MHz, $\text{DMSO-}d_6$): δ 3.20 (s, 3H, NCH_3), 7.10 (d, $J = 7.4$ Hz, 1H, H-9), 7.65–7.75 (m, 2H, H-7 and H-8), 7.80–7.85 (m, 2H, H-2' and H-6'), 8.00–8.05 (m, 3H, H-6, H-3', and H-5').

4-Methyl-1-[2-(trifluoromethyl)phenyl]-1,4-dihydropyrazolo[4,3-c][1,2]benzothiazine-3-carboxylic Acid 5,5-Dioxide (8n). Following the general procedure method B, compound 8n was obtained from 7n in 70% yield as a whitish solid: mp 228–230 °C. $^1\text{H NMR}$ (400 MHz, $\text{DMSO-}d_6$): δ 3.15 (s, 3H, NCH_3), 6.60 (d, $J = 7.9$ Hz, 1H, H-9), 7.60 (dt, $J = 1.3$ and 7.9 Hz, 1H, H-8), 7.65 (dt, $J = 1.0$ and 7.7 Hz, 1H, H-7), 7.85 (d, $J = 7.2$ Hz, 1H, H-3'), 7.90–8.00 (m, 3H, H-4', H-5', and H-6'), 8.05 (dd, $J = 1.3$ and 7.6 Hz, 1H, H-6).

1-(3,4-Difluorophenyl)-4-methyl-1,4-dihydropyrazolo[4,3-c]-[1,2]benzothiazine-3-carboxylic Acid 5,5-Dioxide (8o). Following the general procedure method B, compound 8o was obtained from 7o in 80% yield as a whitish solid: mp 244–246 °C. $^1\text{H NMR}$ (400 MHz, $\text{DMSO-}d_6$): δ 3.10 (s, 3H, NCH_3), 6.95–7.05 (m, 1H, H-9), 7.35–7.45 (m, 1H, H-6'), 7.60–7.75 (m, 3H, H-7, H-8, and H-2'), 7.85–7.90 (m, 1H, H-5'), 7.95–8.00 (m, 1H, H-6), 13.50 (bs, 1H, COOH).

1-(3,4-Dichlorophenyl)-4-methyl-1,4-dihydropyrazolo[4,3-c][1,2]benzothiazine-3-carboxylic Acid 5,5-Dioxide (8p). Following the general procedure method B, compound 8p was obtained from 7p in 90% yield as a whitish solid: mp 245–247 °C. $^1\text{H NMR}$ (400 MHz, $\text{DMSO-}d_6$): δ 3.15 (s, 3H, NCH_3), 7.15 (dd, $J = 1.5$ and 7.5 Hz, 1H, H-9), 7.55 (dd, $J = 2.6$ and 8.7 Hz, 1H, H-6'), 7.65–7.80 (m, 2H, H-7 and H-8), 7.85 (d, $J = 8.7$ Hz, 1H, H-5'), 7.90–8.05 (m, 2H, H-6 and H-2').

1-(3,4-Dimethylphenyl)-4-methyl-1,4-dihydropyrazolo[4,3-c][1,2]benzothiazine-3-carboxylic Acid 5,5-Dioxide (8q). Following the general procedure method B, compound 8q was obtained from 7q in 80% yield as a whitish solid: mp 258–260 °C. $^1\text{H NMR}$ (400 MHz, $\text{DMSO-}d_6$): δ 2.25 and 2.30 (s, each 3H, CH_3), 3.15 (s, 3H, NCH_3), 6.90 (d, $J = 7.6$ Hz, 1H, H-9), 7.23 (dd, $J = 2.0$ and 7.9 Hz, 1H, H-6'), 7.30–7.35 (m, 2H, H-2' and H-5'), 7.60–7.70 (m, 2H, H-7 and H-8), 7.90 (d, $J = 7.6$ Hz, 1H, H-6).

1-(3-Chloro-4-methylphenyl)-4-methyl-1,4-dihydropyrazolo[4,3-c][1,2]benzothiazine-3-carboxylic Acid 5,5-Dioxide (8r). Following the general procedure method B, compound 8r was obtained from 7r in 80% yield as a whitish solid: mp 244–246 °C. $^1\text{H NMR}$ (400 MHz, $\text{DMSO-}d_6$): δ 2.40 (s, 3H, CH_3), 3.20 (s, 3H, NCH_3), 7.00 (d, $J = 7.5$ Hz, 1H, H-9), 7.35–7.40 (m, 1H, H-6'), 7.55 (d, $J = 7.5$ Hz, 1H, H-5'), 7.60–7.70 (m, 3H, H-7, H-8, and H-2'), 7.90–8.00 (m, 1H, H-6).

1-[4-Chloro-3-(trifluoromethyl)phenyl]-4-methyl-1,4-dihydropyrazolo[4,3-c][1,2]benzothiazine-3-carboxylic Acid 5,5-Dioxide (8s). Following the general procedure method B, compound 8s was obtained from 7s in 75% yield as a whitish solid: mp 242–244 °C. $^1\text{H NMR}$ (400 MHz, $\text{DMSO-}d_6$): δ 3.15 (s, 3H, NCH_3), 7.10 (d, $J = 7.7$ Hz, 1H, H-9), 7.60–7.75 (m, 2H, H-7 and H-8), 7.84 (dd, $J = 2.4$ and 8.6 Hz, 1H, H-6'), 7.90 (d, $J = 8.6$ Hz, 1H, H-5'), 8.00 (dd, $J = 1.0$ and 7.3 Hz, 1H, H-6), 8.10 (d, $J = 2.4$ Hz, 1H, H-2'), 13.75 (bs, 1H, COOH).

1-Cyclohexyl-4-methyl-1,4-dihydropyrazolo[4,3-c][1,2]benzothiazine-3-carboxylic Acid 5,5-Dioxide (8t). Following the general procedure method B, compound 8t was obtained from 7t in 70% yield as a white solid: mp 229–231 °C. $^1\text{H NMR}$ (200 MHz, CDCl_3): δ 1.30–1.70 (m, 4H, Cy-CH_2), 2.00–2.45 (m, 6H, Cy-CH_2), 3.30 (s, 3H, NCH_3), 4.50–4.75 (m, 1H, Cy-CH), 7.60–7.90 (m, 3H, H-7, H-8, and H-9), 8.10 (d, $J = 7.7$ Hz, 1H, H-6).

4-Methyl-1,4-dihydropyrazolo[4,3-c][1,2]benzothiazine-3-carboxylic Acid 5,5-Dioxide (8u). Following the general procedure method B, compound 8u was obtained from 7u in 84% yield as yellow solid: mp 169–172 °C. $^1\text{H NMR}$ (400 MHz, $\text{DMSO-}d_6$): δ 3.10 (s, 3H, NCH_3), 7.60–7.65 (m, 1H, H-8), 7.80–7.95 (m, 2H, H-7 and H-9), 8.05 (d, $J = 7.7$ Hz, 1H, H-6), 14.50 (s, 1H, pyrazolo-NH).

General Procedure for Amidation Reaction with *N*-(4-aminophenyl)methanesulfonamide. Method C. A mixture of the acid intermediates 8a–u (1 mmol) in an excess of SOCl_2 was refluxed under stirring for 1 h. The solvent was distilled under reduced pressure, and the residues were washed three times with dry benzene. The corresponding pyrazolobenzothiazine-3-carbonyl chloride was

the general procedure method C, compound **2s** was obtained, from **8s**, in 50% yield as a white solid: mp 288–290 °C. ¹H NMR (400 MHz, DMSO-*d*₆): δ 2.95 (s, 3H, SO₂CH₃), 3.20 (s, 3H, NCH₃), 7.10–7.20 (m, 3H, H-9, H-3", and H-5"), 7.65–7.80 (m, 4H, H-7, H-8, H-2", and H-6"), 7.85 (dd, *J* = 2.5 and 8.6 Hz, 1H, H-6'), 7.95 (d, *J* = 8.6 Hz, 1H, H-5'), 8.00 (dd, *J* = 1.2 and 7.4 Hz, 1H, H-9), 8.25 (d, *J* = 2.5 Hz, 1H, H-2'), 9.60 (s, 1H, SO₂NH), 10.50 (s, 1H, CONH). ¹³C NMR (DMSO-*d*₆): δ 39.08, 39.34, 121.25, 122.22, 122.68 (q, *J*_{C-F} = 272 Hz, CF₃), 123.14, 125.17, 125.28, 125.60–125.70 (m, C-2'), 127.11, 128.63 (q, *J*_{C-F} = 31.4 Hz, C-3'), 130.70, 130.86, 130.89, 131.28 (bs, C-5'), 132.35 (bs, C-4'), 133.60, 133.74, 134.78, 134.93, 138.25, 140.15, 158.58. Anal. Calcd for C₂₅H₁₉ClF₃N₅O₅S₂: C, 47.96; H, 3.06; N, 11.19. Found: C, 47.76; H, 3.18; N, 11.02.

1-Cyclohexyl-4-methyl-*N*-[4-[(methylsulfonyl)amino]phenyl]-1,4-dihydropyrazolo[4,3-*c*][1,2]benzothiazine-3-carboxamide 5,5-Dioxide (2t). Following the general procedure method C, compound **2t** was obtained, from **8t**, as a white solid in 40% yield after purification by flash column chromatography eluting with CHCl₃/MeOH (95:5): mp 254–256 °C. ¹H NMR (400 MHz, DMSO-*d*₆): δ 1.25–1.35 (m, 2H, Cy-CH₂), 1.50–1.65 (m, 2H, Cy-CH₂), 1.70–1.80 (m, 2H, Cy-CH₂), 1.85–1.95 (m, 4H, Cy-CH₂), 2.95 (s, 3H, SO₂CH₃), 3.25 (s, 3H, NCH₃), 4.70–4.80 (m, 1H, Cy-CH), 7.15–7.25 (m, 2H, H-3" and H-5"), 7.70–7.85 (m, 3H, H-8, H-2", and H-6"), 7.90–8.05 (m, 3H, H-6, H-7, and H-9), 9.60 (s, 1H, SO₂NH), 10.10 (s, 1H, CONH). ¹³C NMR (DMSO-*d*₆): δ 25.05, 25.15, 32.93, 38.99, 39.35, 60.63, 121.22, 122.29, 123.77, 124.90, 125.28, 125.55, 130.20, 130.25, 131.17, 134.15, 134.61, 135.02, 137.59, 159.07. Anal. Calcd for C₂₄H₂₇N₅O₅S₂: C, 54.43; H, 5.14; N, 13.22. Found: C, 54.63; H, 5.34; N, 13.01.

4-Methyl-*N*-[4-[(Methylsulfonyl)amino]phenyl]-1,4-dihydropyrazolo[4,3-*c*][1,2]benzothiazine-3-carboxamide 5,5-Dioxide (2u). Following the general procedure method C, compound **2u** was obtained from **8u** as yellow solid in 60% yield after purification by flash column chromatography, eluting with CHCl₃/acetone (6:4): mp 298–299 °C. ¹H NMR (400 MHz, DMSO-*d*₆): δ 3.00 (s, 3H, SO₂CH₃), 3.40 (s, 3H, NCH₃), 7.15–7.20 (m, 2H, H-3" and H-5"), 7.70–7.80 (m, 3H, H-8, H-2", and H-6"), 7.85–7.95 (m, 2H, H-7 and H-9), 8.05 (d, *J* = 7.7 Hz, 1H, H-6'), 9.50 (bs, 1H, SO₂NH), 10.40 (s, 1H, CONH), 14.50 (s, 1H, NH). ¹³C NMR (DMSO-*d*₆): δ 39.22, 39.35, 114.70, 115.50, 121.41, 121.90, 124.30, 124.56, 124.78, 127.13, 130.34, 130.52, 133.78, 134.45, 135.34, 159.10. Anal. Calcd for C₁₈H₁₇N₅O₄S₂: C, 50.10; H, 3.97; N, 16.23. Found: C, 49.90; H, 3.76; N, 16.52.

1-(3-Fluorophenyl)-4-methyl-*N*-phenyl-1,4-dihydropyrazolo[4,3-*c*][1,2]benzothiazine-3-carboxamide 5,5-Dioxide (3). The title compound was prepared following the general procedure method C. Starting from compound **9**¹⁷ and replacing the *N*-(4-aminophenyl)methanesulfonamide with the aniline, compound **3** was obtained as a white solid in 70% yield after purification by flash chromatography, eluting with CHCl₃/MeOH (95:5): mp 202–204 °C. ¹H NMR (400 MHz, DMSO-*d*₆): δ 3.25 (s, 3H, NCH₃), 7.05 (dd, *J* = 1.2 and 7.6 Hz, 1H, H-9), 7.10 (t, *J* = 7.4 Hz, 1H, H-4'), 7.35 (t, *J* = 7.5 Hz, 2H, H-3" and H-5"), 7.45 (dd, *J* = 1.0 and 7.9 Hz, 1H, H-6'), 7.55 (dt, *J* = 1.8 and 8.5 Hz, 1H, H-4'), 7.65–7.75 (m, 4H, H-7, H-8, H-2", and H-6"), 7.80–7.85 (m, 2H, H-2' and H-6'), 8.05 (dd, *J* = 1.8 and 7.8 Hz, 1H, H-6), 10.30 (s, 1H, NH). ¹³C NMR (DMSO-*d*₆): δ 39.15, 113.88 (d, *J*_{C-F} = 25 Hz, C-2'), 117.55 (d, *J*_{C-F} = 21 Hz, C-4'), 121.12, 122.44 (d, *J*_{C-F} = 3 Hz, C-6'), 123.36, 124.55, 124.91, 125.17, 126.79, 129.08, 130.61, 130.74, 130.86, 132.28 (d, *J*_{C-F} = 9.1 Hz, C-5'), 133.47, 138.63, 139.76, 140.51 (d, *J*_{C-F} = 10.2 Hz, C-1'), 158.88, 162.74 (d, *J*_{C-F} = 245.3 Hz, C-3'). Anal. Calcd for C₂₃H₁₇FN₄O₃S: C, 61.60; H, 3.82; N, 12.49. Found: C, 61.72; H, 3.93; N, 12.36.

***N*-[4-(Amino-2-oxoethoxy)phenyl]-1-(3-fluorophenyl)-4-methyl-1,4-dihydropyrazolo[4,3-*c*][1,2]benzothiazine-3-carboxamide 5,5-Dioxide (4).** The title compound was prepared following the general procedure method C. Starting from **9**¹⁷ and replacing the *N*-(4-aminophenyl)methanesulfonamide with the 2-(4-aminophenoxy)acetamide,²¹ compound **4** was obtained as a white solid in 60% yield after purification by flash column chromatography, eluting with CH₂Cl₂/MeOH (98:2): mp 223–225 °C. ¹H NMR (400 MHz, DMSO-*d*₆): δ 3.35 (s, 3H, NCH₃), 4.50 (s, 2H, OCH₂), 6.90–

7.00 (m, 2H, H-3" and H-5"), 7.05 (d, *J* = 7.7 Hz, 1H, H-9), 7.40 (bs, 1H, NH), 7.45 (dd, *J* = 1.8 and 7.3 Hz, 1H, H-4'), 7.50–7.55 (m, 2H, H-8 and NH), 7.65–7.75 (m, 6H, H-7, H-2', H-5', H-6', H-2", and H-6"), 8.00 (dd, *J* = 1.4 and 7.7 Hz, 1H, H-6), 10.40 (s, 1H, CONH). ¹³C NMR (DMSO-*d*₆): δ 39.16, 67.41, 113.88 (d, *J*_{C-F} = 25 Hz, C-2'), 115.10, 117.53 (d, *J*_{C-F} = 21 Hz, C-4'), 122.47 (bs, C-6'), 122.63, 123.37, 124.90, 125.16, 126.70, 130.57, 130.72, 130.84, 132.19, 132.28 (d, *J*_{C-F} = 9 Hz, C-5'), 133.47, 139.86, 140.53 (d, *J*_{C-F} = 10.3 Hz, C-1'), 154.76, 158.56, 162.73 (d, *J*_{C-F} = 245.4 Hz, C-3'). Anal. Calcd for C₂₅H₂₀FN₅O₃S: C, 57.58; H, 3.87; N, 13.43. Found: C, 57.72; H, 4.02; N, 13.15.

1-(3-Fluorophenyl)-4-methyl-1,4-dihydropyrazolo[4,3-*c*][1,2]benzothiazin-3-amine 5,5-Dioxide (10). A mixture of the acid intermediate **9**¹⁷ (1.48 g, 4.0 mmol) in an excess of SOCl₂ (4 mL) was refluxed under stirring for 1 h. The solvent was distilled off, and the residue was washed three times with dry benzene. The corresponding pyrazolobenzothiazine-3-carbonyl chloride was immediately dissolved in acetone (4 mL) and added dropwise to aqueous Na₃N (1 M, 5.6 mL) at 0 °C. After the mixture was stirred at room temperature for 5 min, water was added and the precipitated pinkish solid was filtered. The crude product was immediately suspended into a mixture of toluene/37% HCl (1:1) (20 mL) and heated at 100 °C for 1.5 h. The mixture was then cooled and the solid formed was filtered to give compound **10** (0.95 g, 80%) as a white solid, used as is in the next reaction step: mp 185–187 °C. ¹H NMR (400 MHz, DMSO-*d*₆): δ 3.00 (s, 3H, NCH₃), 6.25 (s, 2H, NH₂), 7.15–7.20 (m, 2H, H-9 and H-4'), 7.25–7.30 (m, 2H, H-2' and H-5'), 7.50–7.55 (m, 1H, H-6'), 7.65–7.70 (m, 2H, H-7 and H-8), 7.95–8.00 (m, 1H, H-6).

***N*-[1-(3-Fluorophenyl)-4-methyl-5,5-dioxido-1,4-dihydropyrazolo[4,3-*c*][1,2]benzothiazin-3-yl]-4-nitrobenzamide (11).** To a stirred solution of amine derivative **10** (0.76 g, 2.3 mmol) in dry pyridine (10 mL), under nitrogen flux, a solution of 4-nitrobenzoyl chloride (0.85 g, 4.6 mmol) in dry pyridine (10 mL) was added dropwise. The mixture was heated at 40 °C for 18 h and then was concentrated to half volume and poured into ice–water, acidified with 2 N HCl (pH 3), and the precipitate formed was filtered under vacuum. The solid was suspended in 20% NaHCO₃, filtered, and purified by flash column chromatography, eluting with CH₂Cl₂/MeOH (95:5) to give compound **11** (0.43 g, 45%) as a white solid: mp 273–275 °C. ¹H NMR (200 MHz, DMSO-*d*₆): δ 3.00 (s, 3H, NCH₃), 7.15 (d, *J* = 6.5 Hz, 1H, H-9), 7.25–7.30 (m, 1H, H-4'), 7.40–7.50 (m, 2H, H-2' and H-5'), 7.55–7.70 (m, 3H, H-7, H-8, and H-6'), 7.90–8.00 (m, 1H, H-6), 8.15–8.25 (m, 2H, H-2" and H-6"), 8.30–8.40 (m, 2H, H-3" and H-5"), 11.05 (s, 1H, CONH).

4-Amino-*N*-[1-(3-fluorophenyl)-4-methyl-5,5-dioxido-1,4-dihydropyrazolo[4,3-*c*][1,2]benzothiazin-3-yl]benzamide (12). A stirred solution of nitro derivative **11** (0.40 g, 0.8 mmol) in DMF (50 mL) was hydrogenated over a catalytic amount of Raney nickel at room temperature and atmospheric pressure for 2 h. The mixture was then filtered over Celite. The filtrate was evaporated to dryness and triturated with ethanol to give the amino derivative **12** (0.26 g, 66%) as a white solid: mp 218–220 °C. ¹H NMR (400 MHz, DMSO-*d*₆): δ 3.00 (s, 3H, NCH₃), 5.80 (s, 2H, NH₂), 6.55–6.65 (m, 2H, H-3" and H-5"), 7.10–7.15 (m, 1H, H-9), 7.30–7.35 (m, 1H, H-4'), 7.40–7.50 (m, 2H, H-2' and H-5'), 7.55–7.70 (m, 3H, H-7, H-8, and H-6'), 7.75–7.80 (m, 2H, H-2" and H-6"), 7.95–8.00 (m, 1H, H-6), 10.15 (s, 1H, CONH).

***N*-[1-(3-Fluorophenyl)-4-methyl-5,5-dioxido-1,4-dihydropyrazolo[4,3-*c*][1,2]benzothiazin-3-yl]-4-(methylsulfonyl)aminobenzamide (5).** Methanesulfonyl chloride (0.2 mL, 3 mmol) was added dropwise to a solution of the amino derivative **12** (0.28 g, 0.6 mmol) in dry CH₂Cl₂ (20 mL) and dry pyridine (2 mL) at 0 °C. The mixture was left overnight at room temperature and then poured into ice/water, acidified with 2 N HCl (pH 3), and extracted with CH₂Cl₂ (4 times). The combined organic layers were washed with brine (2 times), dried, filtered, and evaporated to dryness. The residue was purified by column chromatography, eluting with CH₂Cl₂/MeOH (95:5), affording the target compound **5** (0.16 g, 50%) as a white solid: mp 261–263 °C. ¹H NMR (400 MHz, DMSO-*d*₆): δ 3.00 (s, 3H, SO₂CH₃), 3.20 (s, 3H, NCH₃), 7.15 (dd, *J* = 2.0 and 7.5 Hz, 1H, H-9),

7.30–7.40 (m, 3H, H-4', H-3'', and H-5''), 7.45–7.50 (m, 2H, H-2' and H-5'), 7.60–7.75 (m, 3H, H-7, H-8, and H-6'), 7.95–8.10 (m, 3H, H-6, H-2'', and H-6''), 10.25 (bs, 1H, SO₂NH), 10.70 (s, 1H, CONH). ¹³C NMR (DMSO-*d*₆): δ 36.65, 36.75, 112.84 (d, *J*_{C-F} = 24.1 Hz, C-2'), 116.65 (d, *J*_{C-F} = 21.1, C-4'), 118.29, 121.65 (bs, C-6'), 122.20, 123.79, 124.82, 124.96, 127.86, 129.22, 129.92, 130.32, 130.89, 131.24 (d, *J*_{C-F} = 10 Hz, C-5'), 133.33, 140.48, 140.77 (d, *J*_{C-F} = 10 Hz, C-1'), 142.61, 162.72 (d, *J*_{C-F} = 245.1 Hz, C-3'), 166.35. Anal. Calcd for C₂₄H₂₀FN₃O₅S₂: C, 53.23; H, 3.72; N, 12.93. Found: C, 51.43; H, 4.05; N, 12.66.

Computational Methods. Pyrazolobenzothiazine derivative **2a** was built using the Schrödinger Maestro Interface⁴² and then submitted to Polak–Ribiere conjugate gradient minimization [0.0005 kJ/(Å mol) convergence]. The docking of **2a** into the PSI of 3SKE was then performed with the same methodology previously described.²⁸

Molecular dynamics (MD) simulation of **2a**/NSSB complex was run in explicit solvent, using the TIP4P water model⁴³ in a periodic boundary conditions orthorhombic box. Desmond³¹ was used to set up and run the MD simulations. The simulated environment was built using the system builder utility, with the structures being neutralized by Na⁺ and Cl⁻ ions, which were added until a concentration of 0.15 M was reached. The buried regions were solvated using the “solvate pocket” utility. Before the simulations were performed, a series of minimizations and short MD simulations were carried out to relax the model system by means of a relaxation protocol consisting of six stages: (i) minimization with the solute restrained; (ii) minimization without restraints; (iii) simulation (12 ps) in the NVT ensemble using a Berendsen thermostat (10 K) with non-hydrogen solute atoms restrained; (iv) simulation (12 ps) in the NPT ensemble using a Berendsen thermostat (10 K) and a Berendsen barostat (1 atm) with non-hydrogen solute atoms restrained; (v) simulation (24 ps) in the NPT ensemble using a Berendsen thermostat (300 K) and a Berendsen barostat (1 atm) with non-hydrogen solute atoms restrained; (vi) unrestrained simulation (24 ps) in the NPT ensemble using a Berendsen thermostat (300 K) and a Berendsen barostat (1 atm). At this point, a 10 ns long MD simulation was carried out at a temperature of 300 K in the NPT ensemble using a Nose–Hoover chain thermostat and a Martyna–Tobias–Klein barostat (1.01325 bar). The simulation analysis was carried out by means of the Simulation Interaction Diagram utility⁴⁴ embedded in the Schrödinger Suite 2013 update 2.

Vital Stains. Nile Red was obtained from Sigma. Monodansylcadaverine and LipidTOX Red Neutral lipid stain was obtained from life technologies. Huh-9-13 cells were seeded in glass bottom 35 mm culture dishes (Mattek) at a density of 25,000 cells/dish in complete DMEM without G418 at 37 °C and 5% CO₂. The next day medium was replaced with complete DMEM containing either the proper dilution of the compound to be tested or DMSO. The cells were further incubated for 3 days at 37 °C and 5% CO₂, after which the medium was replaced with complete medium without neutral red and either Nile Red (2 μg/mL), monodansylcadaverine (50 μM), or LipidTOX Red Neutral lipid stain (diluted 1/1000). Next, the cells were incubated for an additional 30 min at 37 °C and 5% CO₂ after which the cells were imaged using a laser-scanning SP5 confocal microscope (Leica Microsystems) equipped with a DMI 6000 microscope and an Acousto optical beam splitter. For Nile Red the yellow-gold fluorescence was monitored at an excitation wavelength (λ_{ex}) of 552 nm and an emission wavelength (λ_{em}) of 636 nm. The red fluorescence was monitored at λ_{ex} of 485 nm and λ_{em} of 525 nm. Monodansylcadaverine was imaged at λ_{ex} of 340 nm and λ_{em} of 530 nm, and LipidTOX Red Neutral lipid stain was assessed at λ_{ex} of 577 nm and λ_{em} of 609 nm.

Physicochemical and ADME Properties. Solubility. For thermodynamic and kinetic solubility determination, solutions were shaken in a shaker bath at room temperature for 48 h before the filtration. Determinations were performed in triplicate by LC–UV–MS assay. Quantification of the compound was made by comparison with corresponding calibration curves realized with standard solutions in methanol.

Shake Flask Method for Lipophilicity. The octanol/water partitioning experiment was performed in a test tube. The test tube was filled with 2.5 mL of water and 2.5 mL of octanol to form the shake flask setup. The tested compound was dissolved directly in octanol.

The sample was sealed and then agitated to produce good mixing between the phases. Time required to reach the equilibrium was 10 h. An aliquot was obtained from each of the phases and is analyzed, typically by HPLC, to determine the concentration of selected compound in each phase.

The experimental log *P* was calculate using the following equation:

$$\log P_{\text{oct/wat}} = \log \left(\frac{[\text{solute}]_{\text{octanol}}}{[\text{solute}]_{\text{water}}} \right)$$

LC analysis was performed with a Perkin-Elmer (series 200) instrument equipped with an UV detector (Perkin-Elmer 785A, UV/vis detector). Chromatographic analysis was conducted using a Polaris C18-A column (150 mm × 4.6 mm, 5 μm particle size) at a flow rate of 0.8 mL min⁻¹ with a mobile phase composed of 50% ACN/50% H₂O.

PAMPA Assay. Donor solution (0.5 mM) was prepared by diluting 1 mM dimethylsulfoxide (DMSO) compound stock solution using phosphate buffer (pH 7.4, 0.025 M). Filters were coated with 5 μL of a 1% (w/v) dodecane solution of phosphatidylcholine or 4 μL of brain polar lipid solution (20 mg/mL 16% CHCl₃, 84% dodecane) prepared from CHCl₃ solution, 10% w/v, for intestinal permeability and BBB permeability, respectively. Donor solution (150 μL) was added to each well of the filter plate. To each well of the acceptor plate was added 300 μL of solution (50% DMSO in phosphate buffer). The compound was tested in three different plates on different days. The sandwich was incubated for 5 or 22 h at room temperature under gentle shaking. After the incubation time, the plates were separated and samples were taken from both receiver and donor sides and analyzed using LC with UV detection at 254 nm. LC analyses were performed with a Perkin-Elmer (series 200) instrument equipped with an UV detector (Perkin-Elmer 785A, UV/vis detector). Chromatographic separations were conducted using a Polaris C18-A column (150 mm × 4.6 mm, 5 μm particle size) at a flow rate of 0.8 mL min⁻¹ with a mobile phase composed of 50% ACN/50% H₂O.

Permeability (*P*_{app}) for PAMPA was calculated according to the following equation, obtained from the Wohlsland and Faller⁴⁵ and Sugano et al.⁴⁶ equation with some modification in order to obtain permeability values in cm/s,

$$P_{\text{app}} = \frac{V_D V_A}{(V_D + V_A) A t} - \ln(1 - r)$$

where *V*_A is the volume in the acceptor well, *V*_D is the volume in the donor well (cm³), *A* is the “effective area” of the membrane (cm²), *t* is the incubation time (s), and *r* is the ratio between drug concentration in the acceptor and equilibrium concentration of the drug in the total volume (*V*_D + *V*_A). Drug concentration was estimated by measuring the peak area.

Membrane retention (%) was calculated according to the following equation:

$$\% \text{MR} = \frac{[r - (D + A)]100}{\text{Eq}}$$

where *r* is the ratio between drug concentration in the acceptor and equilibrium concentration and where *D*, *A*, and Eq represent the drug concentration in the donor, acceptor, and equilibrium solution, respectively.

Metabolic Stability. The compound in DMSO solution was incubated at 37 °C for 60 min in 125 mM phosphate buffer (pH 7.4), 5 μL of human liver microsomal protein (0.2 mg/mL), in the presence of a NADPH-generating system at a final volume of 0.5 mL (compound final concentration, 50 μM); DMSO did not exceed 2% (final solution). The reaction was stopped by cooling in ice and adding 1.0 mL of acetonitrile. The reaction mixtures were then centrifuged,

and the parent drug and metabolites were subsequently determined by LC–UV–MS. Chromatographic analyses were performed with an Agilent 1100 LC/MSD VL system (G1946C) (Agilent Technologies, Palo Alto, CA) consisting of a vacuum solvent degassing unit, a binary high-pressure gradient pump, an 1100 series UV detector, and an 1100 MSD model VL benchtop mass spectrometer. Chromatographic separation was obtained using a Varian Polaris C18-A column (150 mm × 4.6 mm, 5 μm particle size) and gradient elution, eluent A being ACN and eluent B consisting of water. The analysis started with 2% of eluent A, which was rapidly increased to 70% in 12 min, then slowly increased to 98% in 20 min. The flow rate was 0.8 mL min⁻¹, and injection volume was 20 μL. The Agilent 1100 series mass spectra detection (MSD) single-quadrupole instrument was equipped with the orthogonal spray API-ES (Agilent Technologies, Palo Alto, CA). Nitrogen was used as nebulizing and drying gas. The pressure of the nebulizing gas, the flow of the drying gas, the capillary voltage, the fragmentor voltage, and the vaporization temperature were set at 40 psi, 9 L/min, 3000 V, 70 V, and 350 °C, respectively. UV detection was monitored at 280 nm. The LC–ESI-MS determination was performed by operating the MSD in the negative ion mode. Spectra were acquired over the scan range *m/z* 100–1500 using a step size of 0.1 μm. The percentage of compound not metabolized was calculated by comparison with reference solutions.

■ ASSOCIATED CONTENT

Supporting Information

Biochemical and biological assays. This material is available free of charge via the Internet at <http://pubs.acs.org>.

■ AUTHOR INFORMATION

Corresponding Authors

*M.L.B.: phone, +39-075-5855157; e-mail, lbarreca@unipg.it.

*N.K.-B.: phone, +1-973-972-8653; e-mail, kaushik@njms.rutgers.edu.

*J.N.: phone, +32 16 3 37353; e-mail, johan.neyts@rega.kuleuven.be.

Notes

The authors declare no competing financial interest.

■ ACKNOWLEDGMENTS

This work was supported by the UMDNJ Foundation and National Institutes of Health Research Grant CA153147 to N.K.-B. We thank Roberto Bianconi, Stijn Delmotte, Katrien Geerts, and Inge Vliegen for excellent technical assistance. We are grateful to Els Vanstreels for assisting with fluorescence microscopy.

■ ABBREVIATIONS USED

RBV, ribavirin; pegIFN- α , pegylated interferon α ; SVR, sustained virological response; DAA, direct-acting antiviral; NSSB, nonstructural 5B; NI, nucleoside inhibitor; NNI, non-nucleoside inhibitor; TSI, thumb site I; TSII, thumb site II; PSI, palm site I; PSII, palm site II; PSIII, palm site III; SI, selectivity index; MTS, 3-(4,5-dimethylthiazol-2-yl)-5-(3-carboxymethoxyphenyl)-2-(4-sulfophenyl)-2H-tetrazolium; EMCV, encephalomyocarditis virus; IRES, internal ribosome entry site; neo, neomycin phosphotransferase; MDC, monodansylcadaverine; PAMPA, parallel artificial membrane permeability; MR, membrane retention; HLM, human liver microsomes

■ REFERENCES

- (1) Lavanchy, D. Evolving epidemiology of hepatitis C virus. *Clin. Microbiol. Infect.* **2011**, *17*, 107–115.
- (2) Tran, T. T. Overview of epidemiology, diagnosis, and disease progression associated with hepatitis C. *Am. J. Managed Care* **2012**, *18*, S335–S339.
- (3) Fauvelle, C.; Lepiller, Q.; Felmlee, D. J.; Fofana, I.; Habersetzer, F.; Stoll-Keller, F.; Baumert, T. F.; Fafi-Kremer, S. Hepatitis C virus vaccines—progress and perspectives. *Microb. Pathog.* **2013**, *58*, 66–72.
- (4) Berman, K.; Kwo, P. Y. Boceprevir, an NS3 protease inhibitor of HCV. *Clin. Liver Dis.* **2009**, *13*, 429–439.
- (5) Kwong, A. D.; Kauffman, R. S.; Hurter, P.; Mueller, P. Discovery and development of telaprevir: an NS3-4A protease inhibitor for treating genotype 1 chronic hepatitis C virus. *Nat. Biotechnol.* **2011**, *29*, 993–1003.
- (6) Ferenci, P.; Reddy, K. R. Impact of HCV protease-inhibitor-based triple therapy for chronic HCV genotype 1 infection. *Antiviral Ther.* **2011**, *16*, 1187–1201.
- (7) Manns, M. P.; von Hahn, T. Novel therapies for hepatitis C—One pill fits all? *Nat. Rev. Drug Discovery* **2013**, *12*, 595–610.
- (8) Poordad, F.; Lawitz, E.; Kowdley, K. V.; Cohen, D. E.; Podsadecki, T.; Siggelkow, S.; Heckaman, M.; Larsen, L.; Menon, R.; Koev, G.; Tripathi, R.; Pilot-Matias, T.; Bernstein, B. Exploratory study of oral combination antiviral therapy for hepatitis C. *N. Engl. J. Med.* **2013**, *368*, 45–53.
- (9) Liang, T. J.; Ghany, M. G. Current and future therapies for hepatitis C virus infection. *N. Engl. J. Med.* **2013**, *368*, 1907–1917.
- (10) HCV Drugs in Development, October 1, 2013; HCV Advocate, San Francisco, CA. http://www.hcvadvocate.org/hepatitis/hepC/Quick_Ref_Guide.pdf (accessed October 31, 2013).
- (11) Behrens, S. E.; Tomei, L.; De Francesco, R. Identification and properties of the RNA-dependent RNA polymerase of hepatitis C virus. *EMBO J.* **1996**, *15*, 12–22.
- (12) Sofia, M. J.; Chang, W.; Furman, P. A.; Mosley, R. T.; Ross, B. S. Nucleoside, nucleotide, and non-nucleoside inhibitors of hepatitis C virus NSSB RNA-dependent RNA-polymerase. *J. Med. Chem.* **2012**, *55*, 2481–2531.
- (13) Barreca, M. L.; Iraci, N.; Manfroni, G.; Cecchetti, V. Allosteric inhibition of the hepatitis C virus NSSB polymerase: in silico strategies for drug discovery and development. *Future Med. Chem.* **2011**, *3*, 1027–1055.
- (14) Li, H.; Shi, S. T. Non-nucleoside inhibitors of hepatitis C virus polymerase: current progress and future challenges. *Future Med. Chem.* **2010**, *2*, 121–141.
- (15) Manfroni, G.; Meschini, F.; Barreca, M. L.; Leyssen, P.; Samuele, A.; Iraci, N.; Sabatini, S.; Massari, S.; Maga, G.; Neyts, J.; Cecchetti, V. Pyridobenzothiazole derivatives as new chemotype targeting the HCV NSSB polymerase. *Bioorg. Med. Chem.* **2012**, *20*, 866–876.
- (16) Manfroni, G.; Cannalire, R.; Barreca, M. L.; Kaushik-Basu, N.; Leyssen, P.; Winkvist, J.; Iraci, N.; Manvar, D.; Paeshuyse, J.; Guhamazumder, R.; Basu, A.; Sabatini, S.; Tabarrini, O.; Danielson, U. H.; Neyts, J.; Cecchetti, V. The versatile nature of the 6-aminoquinolone scaffold: identification of submicromolar hepatitis C virus NSSB inhibitors. *J. Med. Chem.* **2014**, *57*, 1952–1963.
- (17) Barreca, M. L.; Manfroni, G.; Leyssen, P.; Winkvist, J.; Kaushik-Basu, N.; Paeshuyse, J.; Krishnan, R.; Iraci, N.; Sabatini, S.; Tabarrini, O.; Basu, A.; Danielson, U. H.; Neyts, J.; Cecchetti, V. Structure-based discovery of pyrazolobenzothiazine derivatives as inhibitors of hepatitis C virus replication. *J. Med. Chem.* **2013**, *56*, 2270–2282.
- (18) Shaw, A. N.; Tedesco, R.; Bambal, R.; Chai, D.; Concha, N. O.; Darcy, M. G.; Dhanak, D.; Duffy, K. J.; Fitch, D. M.; Gates, A.; Johnston, V. K.; Keenan, R. M.; Lin-Goerke, J.; Liu, N.; Sarisky, R. T.; Wiggall, K. J.; Zimmerman, M. N. Substituted benzothiadiazine inhibitors of hepatitis C virus polymerase. *Bioorg. Med. Chem. Lett.* **2009**, *19*, 4350–4353.
- (19) Cecchetti, V.; Fravolini, A.; Schiaffella, F.; De Regis, M.; Orzalesi, G.; Volpato, I. Synthesis and pharmacologic activity of the carboxamides of pyrazolo-1,2-benzothiazine and isoxazolo-1,2-benzothiazinecarboxamides. *Farmaco* **1983**, *38*, 35–44.
- (20) Waslei, J.; Rosenthal, G. J.; Sun, X.; Strong, S.; Qiu, J. Novel Pyrrole Inhibitors of S-Nitrosoglutathione Reductase as Therapeutic Agents. PTC WO 2010/019903 A1, 2010.

- (21) Singh, R.; Argade, A.; Payan, D.; Molineaux, S.; Holland, S. J.; Clough, J.; Keim, H.; Bhamipidati, S.; Sylvain, C.; Li, H.; Rossi, A. B. 2,4-Pyrimidine Compounds and Their Uses. U.S. 2005/0209230 A1, 2005.
- (22) Nichols, D. B.; Fournet, G.; Gurukumar, K. R.; Basu, A.; Lee, J. C.; Sakamoto, N.; Kozielski, F.; Musmuca, I.; Joseph, B.; Ragno, R.; Kaushik-Basu, N. Inhibition of hepatitis C virus NSSB polymerase by S-trityl-L-cysteine derivatives. *Eur. J. Med. Chem.* **2012**, *49*, 191–199.
- (23) Kaushik-Basu, N.; Bopda-Waffo, A.; Talele, T. T.; Basu, A.; Costa, P. R.; da Silva, A. J.; Sarafianos, S. G.; Noel, F. Identification and characterization of coumestans as novel HCV NSSB polymerase inhibitors. *Nucleic Acids Res.* **2008**, *36*, 1482–1496.
- (24) Chen, Y.; Bopda-Waffo, A.; Basu, A.; Krishnan, R.; Silberstein, E.; Taylor, D. R.; Talele, T. T.; Arora, P.; Kaushik-Basu, N. Characterization of aurintricarboxylic acid as a potent hepatitis C virus replicase inhibitor. *Antiviral Chem. Chemother.* **2009**, *20*, 19–36.
- (25) Nichols, D. B.; Leao, R. A.; Basu, A.; Chudayeu, M.; de Moraes Pde, F.; Talele, T. T.; Costa, P. R.; Kaushik-Basu, N. Evaluation of coumarin and neoflavone derivatives as HCV NSSB polymerase inhibitors. *Chem. Biol. Drug Des.* **2013**, *81*, 607–614.
- (26) Cheng, C. C.; Shipp, G. W., Jr.; Yang, Z.; Kawahata, N.; Lesburg, C. A.; Duca, J. S.; Bandouveres, J.; Bracken, J. D.; Jiang, C. K.; Agrawal, S.; Ferrari, E.; Huang, H. C. Inhibitors of hepatitis C virus polymerase: synthesis and characterization of novel 2-oxy-6-fluoro-N-((S)-1-hydroxy-3-phenylpropan-2-yl)-benzamides. *Bioorg. Med. Chem. Lett.* **2010**, *20*, 2119–2124.
- (27) Betzi, S.; Eydoux, C.; Bussetta, C.; Blemont, M.; Leyssen, P.; Debarnot, C.; Ben-Rahou, M.; Haiech, J.; Hibert, M.; Gueritte, F.; Grierson, D. S.; Romette, J. L.; Guillemot, J. C.; Neyts, J.; Alvarez, K.; Morelli, X.; Dutartre, H.; Canard, B. Identification of allosteric inhibitors blocking the hepatitis C virus polymerase NSSB in the RNA synthesis initiation step. *Antiviral Res.* **2009**, *84*, 48–59.
- (28) Barreca, M. L.; Iraci, N.; Manfroni, G.; Gaetani, R.; Guercini, C.; Sabatini, S.; Tabarrini, O.; Cecchetti, V. Accounting for target flexibility and water molecules by docking to ensembles of target structures: the HCV NSSB palm site I inhibitors case study. *J. Chem. Inf. Model.* **2014**, *54*, 481–497.
- (29) Anilkumar, G. N.; Lesburg, C. A.; Selyutin, O.; Rosenblum, S. B.; Zeng, Q.; Jiang, Y.; Chan, T. Y.; Pu, H.; Vaccaro, H.; Wang, L.; Bennett, F.; Chen, K. X.; Duca, J.; Gavalas, S.; Huang, Y.; Pinto, P.; Sannigrahi, M.; Velazquez, F.; Venkatraman, S.; Vibulbhan, B.; Agrawal, S.; Butkiewicz, N.; Feld, B.; Ferrari, E.; He, Z.; Jiang, C. K.; Palermo, R. E.; McMonagle, P.; Huang, H. C.; Shih, N. Y.; Njoroge, G.; Kozlowski, J. A., II; Novel, HCV NSSB polymerase inhibitors: discovery of indole 2-carboxylic acids with C3-heterocycles. *Bioorg. Med. Chem. Lett.* **2011**, *21*, 5336–5341.
- (30) *Glide*, version 6.0; Schrödinger, LLC, New York, NY, 2013.
- (31) *Desmond Molecular Dynamics System*, version 3.5; D. E. Shaw Research: New York, NY, 2013.
- (32) Windisch, M. P.; Frese, M.; Kaul, A.; Tripler, M.; Lohmann, V.; Bartenschlager, R. Dissecting the interferon-induced inhibition of hepatitis C virus replication by using a novel host cell line. *J. Virol.* **2005**, *79*, 13778–13793.
- (33) Stuyver, L. J.; McBrayer, T. R.; Tharnish, P. M.; Hassan, A. E.; Chu, C. K.; Pankiewicz, K. W.; Watanabe, K. A.; Schinazi, R. F.; Otto, M. J. Dynamics of subgenomic hepatitis C virus replicon RNA levels in Huh-7 cells after exposure to nucleoside antimetabolites. *J. Virol.* **2003**, *77*, 10689–10694.
- (34) Vrolijk, J. M.; Kaul, A.; Hansen, B. E.; Lohmann, V.; Haagmans, B. L.; Schalm, S. W.; Bartenschlager, R. A replicon-based bioassay for the measurement of interferons in patients with chronic hepatitis C. *J. Virol. Methods* **2003**, *110*, 201–209.
- (35) Bartenschlager, R.; Lohmann, V. Novel cell culture systems for the hepatitis C virus. *Antiviral Res.* **2001**, *52*, 1–17.
- (36) Kansy, M.; Senner, F.; Gubernator, K. Physicochemical high throughput screening: parallel artificial membrane permeation assay in the description of passive absorption processes. *J. Med. Chem.* **1998**, *41*, 1007–1010.
- (37) Bermejo, M.; Avdeef, A.; Ruiz, A.; Nalda, R.; Ruell, J. A.; Tsinman, O.; González, I.; Fernández, C.; Sánchez, G.; Garrigues, T. M.; Merino, V. PAMPA—a drug absorption in vitro model 7. Comparing rat in situ, Caco-2, and PAMPA permeability of fluorquinolones. *Eur. J. Pharm. Sci.* **2004**, *21*, 429–441.
- (38) Koljonen, M.; Rousu, K.; Cierny, J.; Kaukonen, A. M.; Hirvonen, J. Transport evaluation of salicylic acid and structurally related compounds across Caco-2 cell monolayers and artificial PAMPA membranes. *Eur. J. Pharm. Biopharm.* **2008**, *70*, 531–538.
- (39) Bassendine, M. F.; Sheridan, D. A.; Felmlee, D. J.; Bridge, S. H.; Toms, G. L.; Neely, R. D. HCV and the hepatic lipid pathway as a potential treatment target. *J. Hepatol.* **2011**, *55*, 1428–1440.
- (40) Rasmussen, A. L.; Diamond, D. L.; McDermott, J. E.; Gao, X.; Metz, T. O.; Matzke, M. M.; Carter, V. S.; Belisle, S. E.; Korth, M. J.; Waters, K. M.; Smith, R. D.; Katze, M. G. Systems virology identifies a mitochondrial fatty acid oxidation enzyme, dodecenoyl coenzyme A delta isomerase, required for hepatitis C virus replication and likely pathogenesis. *J. Virol.* **2011**, *85*, 11646–11654.
- (41) Donato, M. T.; Gomez-Lechon, M. J. Drug-induced liver steatosis and phospholipidosis: cell-based assays for early screening of drug candidates. *Curr. Drug Metab.* **2012**, *13*, 1160–1173.
- (42) *Maestro*, version 9.5; Schrödinger, LLC: New York, NY, 2013.
- (43) Jorgensen, W. L.; Chandrasekhar, J.; Madura, J. D.; Impey, R. W.; Klein, M. L. Comparison of simple potential functions for simulating liquid water. *J. Chem. Phys.* **1983**, *79*, 926–935.
- (44) *Maestro-Desmond Interoperability Tools*, version 3.5; Schrödinger: New York, NY, 2013.
- (45) Wohnsland, F.; Faller, B. High-throughput permeability pH profile and high-throughput alkane/water log P with artificial membranes. *J. Med. Chem.* **2001**, *44*, 923–930.
- (46) Sugano, K.; Hamada, H.; Machida, M.; Ushio, H. High throughput prediction of oral absorption: improvement of the composition of the lipid solution used in parallel artificial membrane permeation assay. *J. Biomol. Screening* **2001**, *6*, 189–196.